AD-A130 138 INFRARED CHEMILUMINESCENCE STUDIES OF ION-MOLECULE REACTIONS IN A FLOWING AFTERGLOW(U) COLORADO UNIV AT BOULDER DEPT OF CHEMISTRY V M BIERBAUM ET AL. 1982 1/1

UNCLASSIFIED AFOSR-TR-83-0558 AFOSR-78-3565 F/G 20/5 NL

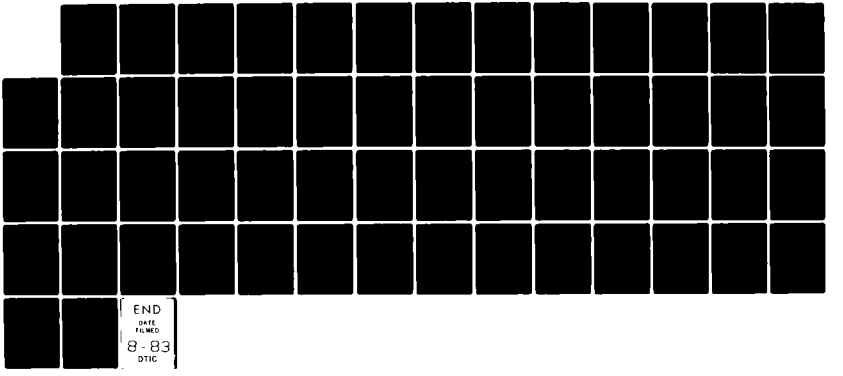

END
DATE FILMED
8-83
DTIC

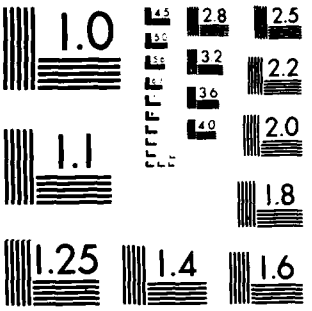

MICROCOPY RESOLUTION TEST CHART
NATIONAL BUREAU OF STANDARDS-1963-A

Unclassified

SECURITY CLASSIFICATION OF THIS PAGE (When Data Entered)

REPORT DOCUMENTATION PAGE		READ INSTRUCTIONS BEFORE COMPLETING FORM
1. REPORT NUMBER **AFOSR-TR- 83-0558**	2. GOVT ACCESSION NO.	3. RECIPIENT'S CATALOG NUMBER
4. TITLE (and Subtitle) Infrared Chemiluminescence Studies of Ion-Molecule Reactions in a Flowing Afterglow		5. TYPE OF REPORT & PERIOD COVERED Final Report
		6. PERFORMING ORG. REPORT NUMBER
7. AUTHOR(s) Veronica M. Bierbaum, Stephen R. Leone, G. Barney Ellison		8. CONTRACT OR GRANT NUMBER(s) AFOSR-78-3565
9. PERFORMING ORGANIZATION NAME AND ADDRESS Department of Chemistry, University of Colorado Boulder, CO 80309		10. PROGRAM ELEMENT, PROJECT, TASK AREA & WORK UNIT NUMBERS 6110&F 2303/B1
11. CONTROLLING OFFICE NAME AND ADDRESS Air Force Office of Scientific Research/NC Attn: Major William G. Thorpe, Directorate of Chemical Sciences, Bldg. 410, Bolling Air Force Base Washington, DC 20332		12. REPORT DATE 1 Apr 78 - 30 Sep 82
		13. NUMBER OF PAGES 56
14. MONITORING AGENCY NAME & ADDRESS (if different from Controlling Office)		15. SECURITY CLASS. (of this report) Unclassified
		15a. DECLASSIFICATION/DOWNGRADING SCHEDULE

16. DISTRIBUTION STATEMENT (of this Report)

Approved for public release; distribution unlimited

17. DISTRIBUTION STATEMENT (of the abstract entered in Block 20, if different from Report)

DTIC ELECTE JUL 5 1983 A

18. SUPPLEMENTARY NOTES

19. KEY WORDS (Continue on reverse side if necessary and identify by block number)

Ion-molecule reactions
Infrared chemiluminescence
Laser-induced fluorescence
Flowing afterglow
Ion-molecule dynamics

20. ABSTRACT (Continue on reverse side if necessary and identify by block number)

A powerful new method has been developed for studying the dynamics of thermal energy ion-molecule reactions. Ion reactions are carried out in a well-characterized, state-of-the-art flowing afterglow apparatus and the excited products are monitored optically. Two complementary techniques are used: direct observation of wavelength dispersed infrared chemiluminescence and laser-induced fluorescence detection, i.e. laser excitation of the product molecules to bound electronic states and detection of the resulting visible fluorescence. The initial vibrational distributions have been determined for products formed in a wide variety of ion-molecule processes, including proton transfer, charge transfer, heavy- (ovdr)

DD FORM 1 JAN 73 1473 EDITION OF 1 NOV 65 IS OBSOLETE

Unclassified

SECURITY CLASSIFICATION OF THIS PAGE (When Data Entered)

20. Abstract (continued):
atom transfer and associative detachment reactions. Information on nascent rotational populations and on vibrational deactivation of ions has also been obtained recently.

Table of Contents

A. Objectives of the Research

The goals of this research project include: the design, construction and characterization of a state-of-the-art flowing afterglow apparatus with infrared chemiluminescence and laser-induced fluorescence detection; determination of the rotational and vibrational energy distributions of the products of thermal energy ion-molecule reactions; studies of the internal excitation of molecular ions in a drift field; measurement of collisional deactivation rates of vibrationally excited species; determination of infrared emission properties and yields of infrared emission from ion-molecule reactions.

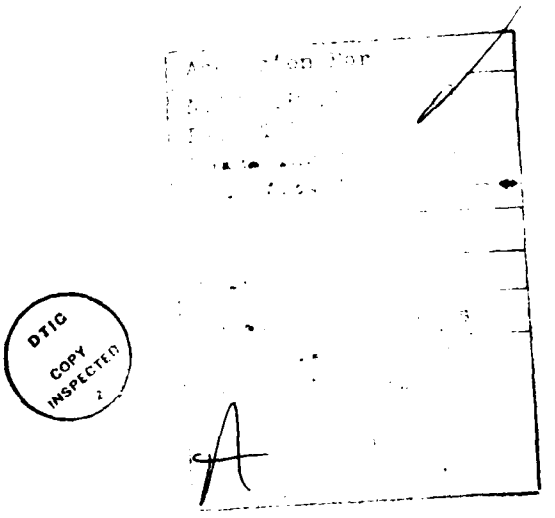

B. Status of the Research Effort

1. The flowing afterglow apparatus

A state-of-the-art flowing afterglow apparatus (Ferguson, et al., 1969, Fehsenfeld, 1975a) with infrared chemiluminescence and laser-induced fluorescence detection capabilities was designed and constructed. This apparatus, shown in Fig. 1, consists of a flow tube in which reactant ions are produced in a flow of buffer gas maintained by a large pumping system. The ion-molecule reactions are carried out by the addition of a neutral reactant. Optical emission in the infrared and by laser-induced fluorescence are detected at various ports just after the neutral addition. The ion population is continuously monitored downstream by a quadrupole mass filter coupled with a particle multiplier.

a. Infrared chemiluminescence

Incorporation of infrared chemiluminescence detection requires three changes to the conventional flowing afterglow (Fig. 1) (Zwier, et al., 1980a): modification of the flow tube to allow collection of light, use of a sensitive infrared detector and associated electronics, and incorporation of a shutter to provide modulation of the ions. The infrared port consists of a 2.5 cm diam NaCℓ window inserted tangent to the inside wall of the flow tube. This recessed design allows close placement of the infrared detector to the flow tube for viewing a volume of up to 120 cm^3. Since the wavelength transmission of interference filters depends on the angle of incidence, larger port-to-detector separations are usually used to minimize collection of off-normal light. A 10 cm focal length aluminum mirror is placed opposite the window and a 5.1 cm diam f/1 CaF_2 lens is used above the window to collect and image the infrared emission onto the detector.

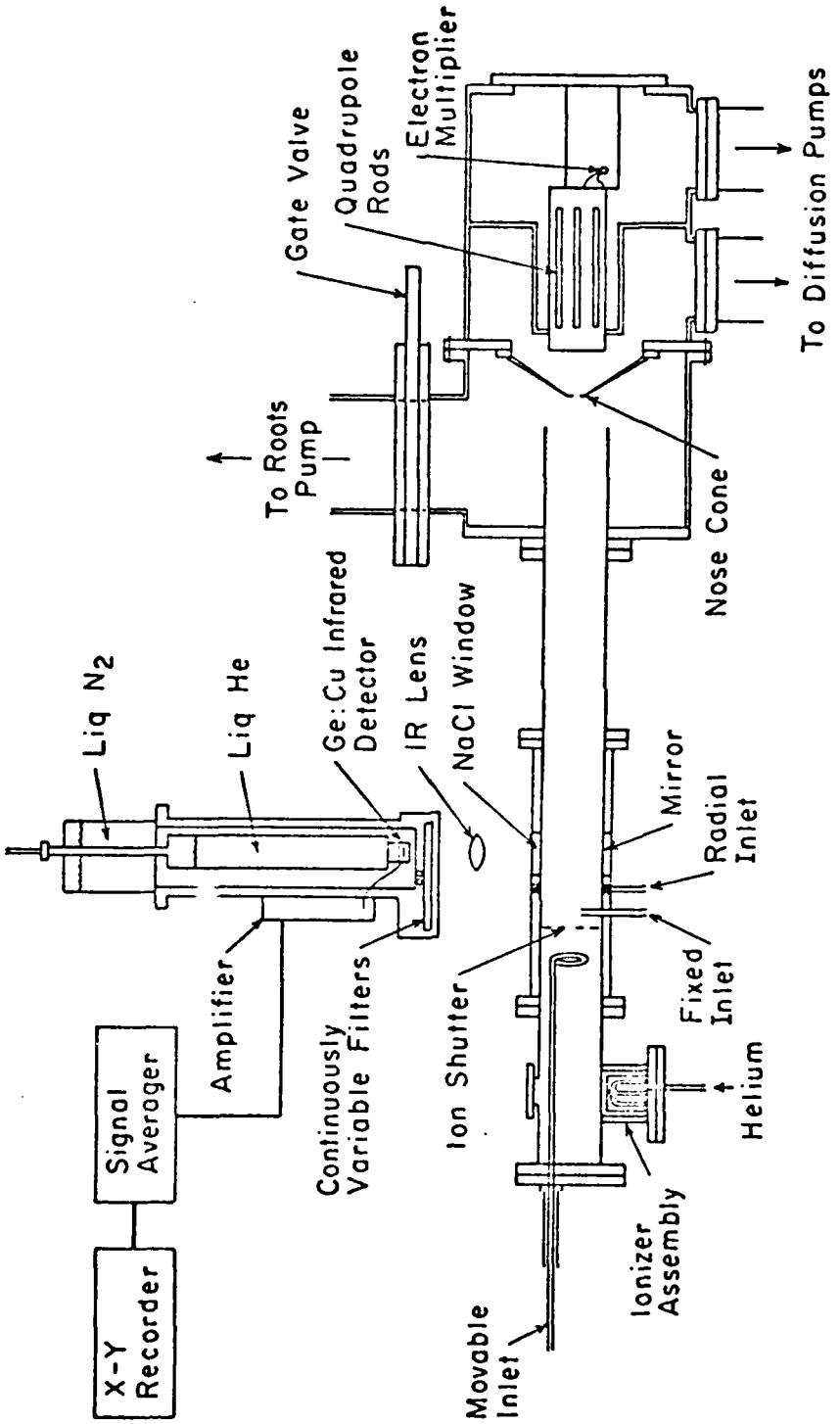

Fig. 1. Schematic drawing of the flowing afterglow, infrared chemiluminescence apparatus.

Two infrared detector assemblies are used in the infrared chemiluminescence experiments, an indium antimonide detector for the reactions of chloride and cyanide ions and a copper-doped-germanium detector for the studies involving fluoride ion and N^+. The photovoltaic InSb detector is a liquid nitrogen cooled, 1.27 cm diam element with a wavelength response of 1.0-5.5 μm and a detectivity, $D^* = 1 \times 10^{11}$ cm $Hz^{1/2}$ W^{-1} at 5 μm. The large area of the detector element, the high D^* value, and the ease of liquid nitrogen cooling make this detector best-suited for initial studies. Wavelength resolution of the transmitted light is provided by a series of room temperature fixed frequency interference filters mounted below the detector. Cold gas filter cells containing HCℓ, HF, or HCN are also employed to selectively absorb more than 99% of the emission from v=1→0. The output of the InSb detector is amplified and modulated signals are accumulated in a signal averager.

The photoconductive Ge:Cu detector is a liquid helium cooled 3 mm × 10 mm element with a wavelength response of 2-30 μm and a detectivity, $D^* \sim 1 \times 10^{12}$ cm $Hz^{1/2}$ W^{-1} at 3 μm, under background limited conditions. Liquid helium cooled magnesium fluoride and/or sapphire windows are mounted directly on the detector heat sink to provide a long-wavelength blackbody cutoff. The detector views emission through a wavelength-selective, low resolution rotatable circular variable interference filter assembly (CVF) and a 1.5 mm × 12 mm slit, both cooled to 77 K (Zwier, et al., 1981). The output of the Ge:Cu detector is amplified by current feedback circuitry and then accumulated in the signal averager.

The circular variable filters consist of three 90° annular sections of a transparent substrate coated with continuously varying thicknesses of multiple dielectrics. Each radial slice through the annulus is a narrow bandpass interference filter whose peak transmission wavelength varies linearly around the

circumference of the annulus. The three filter segments span the range 2.5-14.5 μm and are calibrated to ±0.05 μm using a broadband infrared source and a monochromator. The resolution is slit width limited and varies from 0.055 μm at 2.5 μm to 0.11 μm at 8 μm; signal collection is maximized by this relatively low resolution configuration. The sensitivity of the detector and filter combination as a function of wavelength is measured by chopping and imaging the output of a calibrated blackbody source onto the detector; the output vs CVF setting is normalized to the calculated blackbody emission curve.

The ion source generates a variety of reactive radical and metastable species in addition to the reactant ion of interest. In order to distinguish the desired infrared emission of the ion-molecule reaction from all other interfering signals, the ions must be modulated. Ion modulation is achieved by repetitively applying a repulsive potential to a 95% transmission tungsten mesh stretched across the flow tube about 40 cm downstream of the ionizer. For negative ions the grid is typically pulsed to -10 V for 0.3 msec and returned to ground for the remainder of the 5 or 10 msec period as shown in Fig. 2 for chloride ion. This causes a decrease in the chloride ion density as detected at the quadrupole mass spectrometer 6 msec later, but does not affect the density of uncharged species. If hydrogen iodide is added to this modulated plasma, vibrationally hot HCl product is formed. The decrease in the ion density appears as a decrease in the infrared emission intensity due to the interruption of the ion-molecule reaction, therefore the area of the emission curve is directly proportional to the amount of HCl(v) arising from the ion-molecule reaction. These signals are monitored as a function of transmitted wavelength to construct a spectrum.

In a typical experiment, reactant ions are formed in the ion source, thermalized in a 40 cm section of flow tube, and modulated with the shutter.

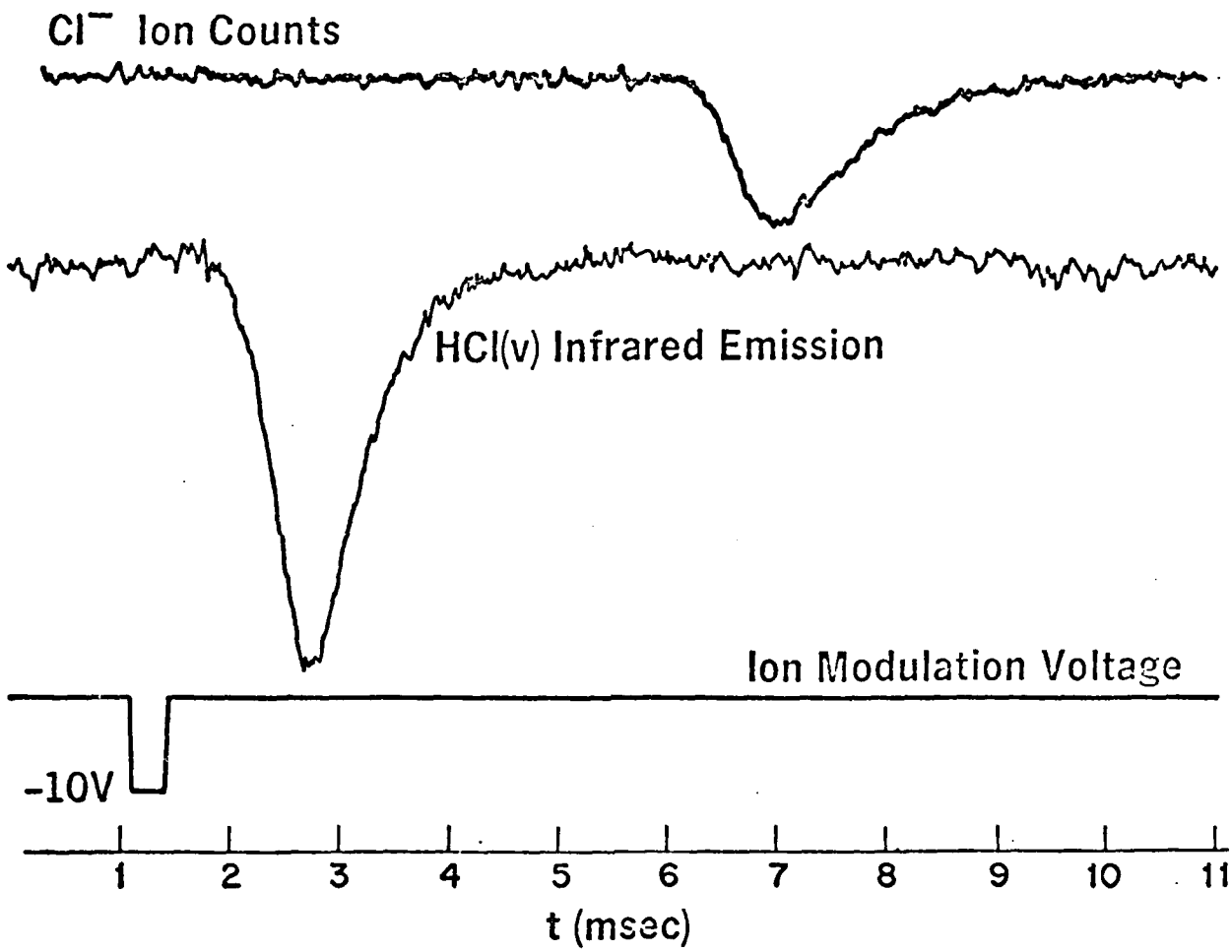

Fig. 2. Ion modulation for infrared chemiluminescence detection. Lower: minus 10 V pulse repetitively applied to the ion shutter. Middle: HCℓ(v) infrared emission, showing a decrease in emission when the ions are stopped and delayed by the flow time between the shutter and IR detector. Upper: Chloride ion counts observed downstream with the quadrupole mass spectrometer when no reactant is added. The spreading of the modulated ion packet is due to axial diffusion [From Zwier, et al., (1980a)].

The addition of neutral reagent 10 cm downstream of the mesh initiates the ion-molecule reaction, and wavelength resolved infrared emission is detected in phase with the ion modulation by the infrared detector positioned 2-5 cm downstream. Signal-to-noise before averaging is about 0.1-1.0, in good agreement with estimates based on ion densities, radiative lifetimes, collection efficiency and detector characteristics. Typically 10^4-10^5 modulation periods are accumulated and averaged at each wavelength, corresponding to 1-10 minutes of data collection. The raw infrared emission intensities are corrected for detector and filter sensitivity and a complete spectrum is constructed (Fig. 3). For fixed interference filter experiments, populations are deduced from the transmission through several filters and the known values of the Einstein coefficients, A_v (Maricq, et al., 1981). For the CVF data the chemiluminescence spectra are computer analyzed by a linear least squares procedure in which relative populations, N_v, are extracted (Zwier, et al., 1981). In those calculations, the molecular line positions, the transition strength of each line, and the spectral resolution are specified. Small corrections to the resulting vibrational populations are then applied to account for radiative and collisional cascading between the time of formation and detection of the vibrationally excited product. In most cases a thermal distribution of rotational states is observed and used in the computer fitting routine. When possible, vibrational surprisal plots are extrapolated to obtain estimates of the v=0 population and of the average fraction of available energy deposited into product vibration (Zwier, et al., 1981).

A variety of experimental checks are performed to insure that the infrared emission arises solely from the ion-molecule reaction of interest and that the vibrational distributions are nascent. Ion modulation with phase sensitive detection of chemiluminescence eliminates contributions from neutral

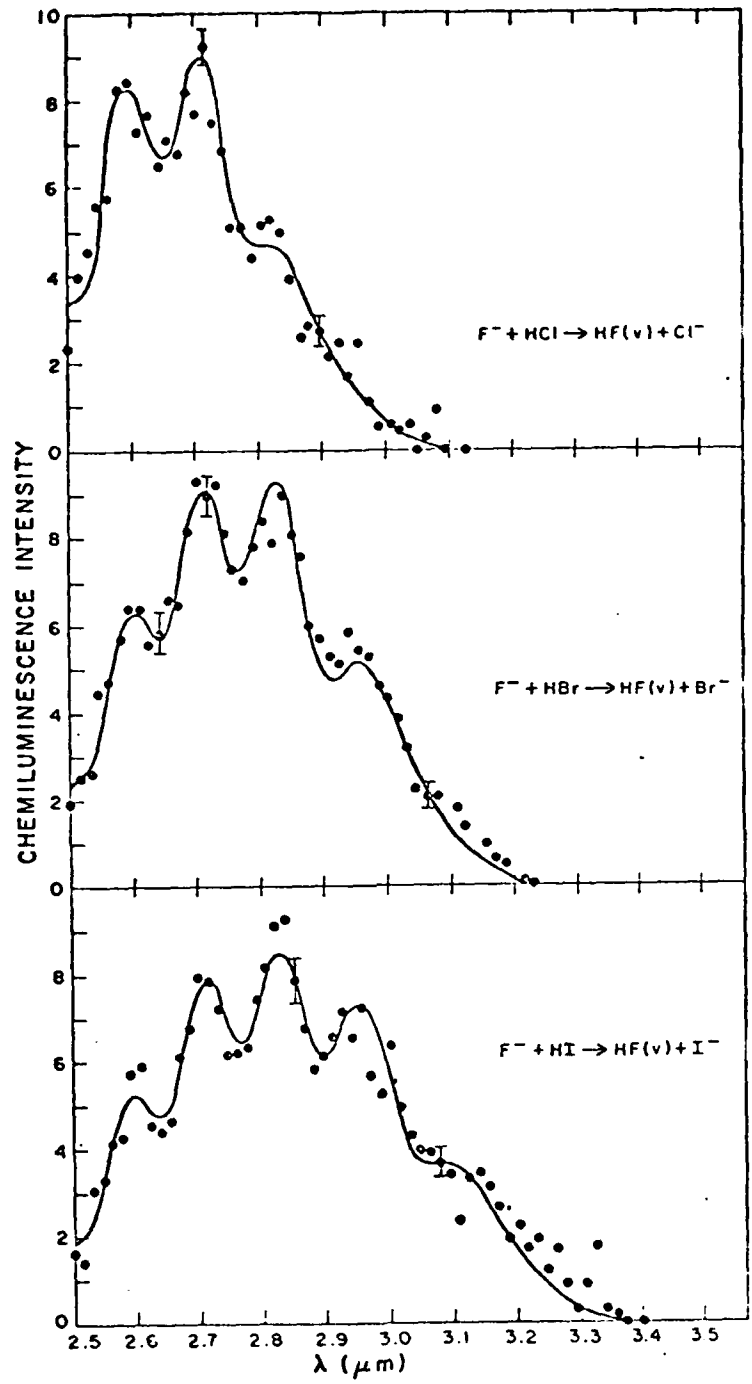

Fig. 3. Low resolution infrared chemiluminescence spectra of HF(v) produced from the ion reactions F^- + HCℓ, HBr, and HI. The anharmonicity of the vibrational levels creates an overlap between P and R branches of adjacent bands, producing the multiple peaked spectrum. The exothermicities are sufficient to produce HF up to v=3, 4, and 5 for the HCℓ, HBr, and HI reactants, respectively. [From Weisshaar, et al. (1981)].

reactions. Ion-molecule reactions are monitored with the mass spectrometer before and after addition of the neutral reagent. In a valid experiment, the reactant species is depleted, the product species is generated, and all other ion signals remain constant. Other evidence that the detected emission arises from the ion reaction is the proper correlation of chemiluminescence intensity with ion density and neutral reactant flow and the correspondence of the time evolution of the infrared emission to that of the ion arrival waveform at the mass spectrometer. In some test experiments, a second mesh is inserted into the flow tube upstream of the ion shutter and held at a constant, highly repulsive potential. This effectively stops all ions and the infrared emission intensity decreases by greater than 98%. Finally, for some reactions (e.g., Cl^- or F^- + HI), the neutral reaction counterpart is known to populate vibrational levels higher than allowed by the ion process exothermicity. Absence of emission in this region confirms that the neutral process does not contribute to the detected infrared signals.

Gas phase deactivation, wall deactivation, and radiative cascading must be considered for quantitative assignment of initial vibrational distributions. Gas phase deactivation is addressed by monitoring infrared emission over a wide range of flow rates of precursor gas and neutral reactant. Data are obtained under experimental conditions where vibrational deactivation is completely negligible or very small. In these latter cases the data are corrected using published collisional relaxation rates. Although vibrational relaxation of many diatomics by helium is extremely inefficient (Leone, 1982), rotational relaxation is rapid on the time scales of our experiment (Sung and Setser, 1978). This is experimentally checked in several ways. For example, in the formation of HCl from Cl^- + HBr where only v=1 is formed, emission is totally blocked by a gas filter, indicating the absence of hot rotational levels. In

other experiments, emission to red or blue wavelengths, which would reflect the presence of non-Boltzmann rotational distributions, is not observed. Moreover, in the computer simulation of emission intensity vs wavelength, a rotational temperature of 300 K gives excellent agreement to the data, assumed temperatures above 450 K result in considerably degraded fits. Therefore vibrational excitation is largely preserved, but rotational relaxation is complete.

Vibrational deactivation at the walls of the flow tube is negligible. Calculations indicate that only 5% of the product species experience a collision with the wall before detection of chemiluminescence. This is supported by the consistency of data obtained with different distances between the neutral inlet and the infrared detector.

Finally, radiative cascading, that is depletion in the population of level v and the resulting increase in the population of level (v-1) by radiative processes, must be carefully evaluated. The raw populations are corrected for the known radiative lifetimes by a simple kinetic model to deduce the initial vibrational populations. Corrections never exceed 20% and are generally considerably smaller.

b. Laser-induced fluorescence

Use of laser-induced fluorescence detection requires several extensions of the flowing afterglow as illustrated in Fig. 4 (Hamilton, et al., 1982): incorporation of the laser; flow tube modifications to allow entry of laser light, collection of fluorescence, and reduction of background light; a photomultiplier tube, lenses and filters to detect the fluorescence; and signal collection and processing electronics.

A Nd:YAG pumped dye laser is used, which is capable of producing tunable pulsed radiation at 0-20 Hz with energies of 5-50 mJ/pulse in the 380-700 nm

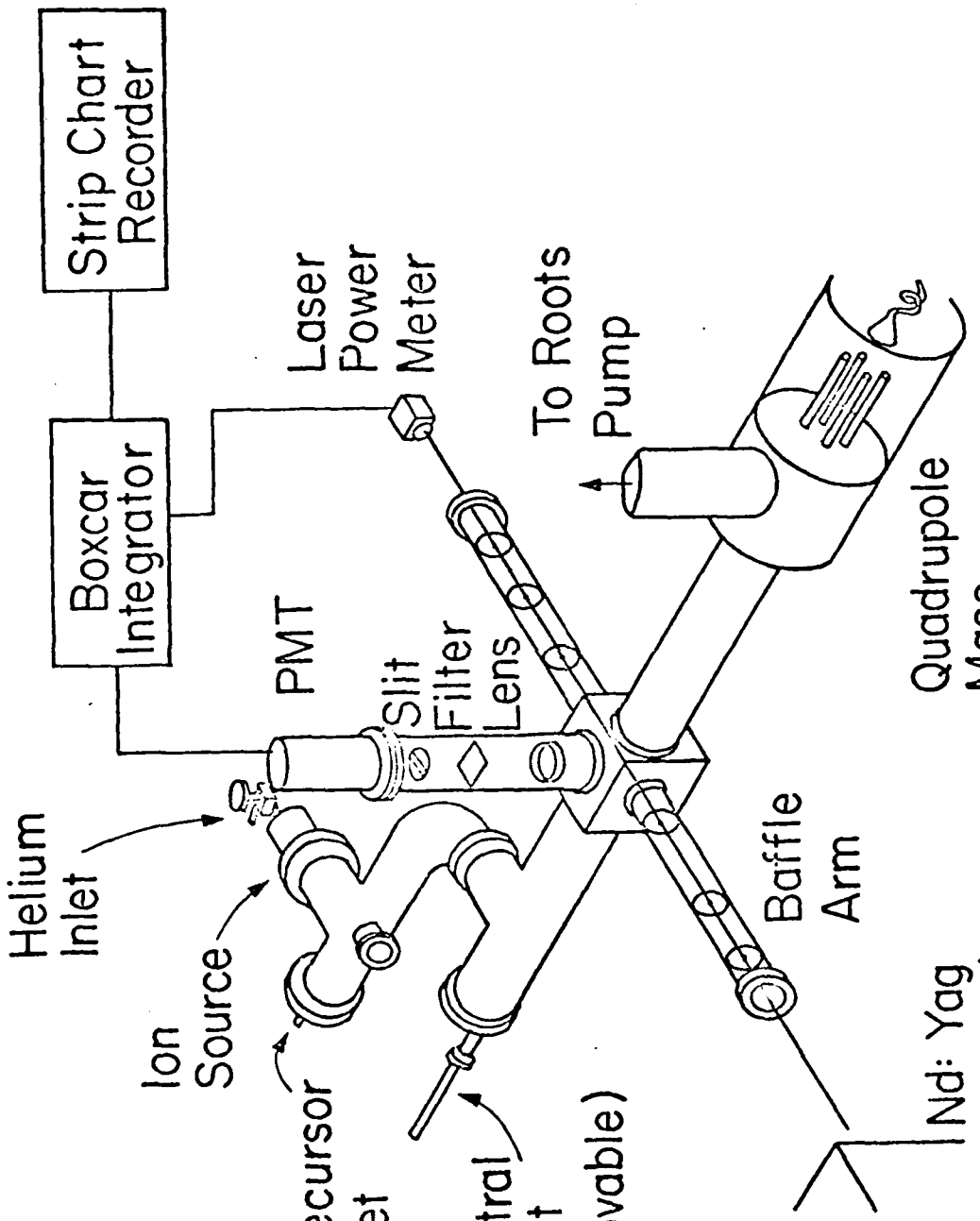

Fig. 4. Flowing afterglow apparatus incorporating laser-induced fluorescence detection.

range. Use of nonlinear optical techniques extends the output range to 217 nm through harmonic generation and mixing in angle phase-matched crystals. Most experiments are performed with 0.1-1 mJ/pulse to avoid saturation of the molecular transition. The short pulse duration of 5 nsec allows gating out of the scattered laser light. Careful control of amplified spontaneous emission is essential to avoid broadband background signals. The full width at half maximum of 0.02 nm provides rotational resolution in most cases. Three species have been studied using laser-induced fluorescence: N_2^+, CO^+, and OH.

A section of flow tube incorporates two sidearms perpendicular to the direction of flow to allow the entrance and exit of laser light and a third port above the flow tube for the collection of fluorescence. Windows are made of UV grade quartz. The baffle arms contain several apertures to reduce scattered laser light. A blackened right angle bend is added to the flow tube between the ionizer and LIF regions to reduce background light from the ion source. The photomultiplier tube is positioned directly above the flow tube in the region of laser probing to detect the resulting fluorescence. The output of the photomultiplier is amplified and fed into a boxcar integrator.

To reduce the background signals, the photomultiplier field of view is restricted to the small volume of gas intersected by the laser beam by a combination lens and slit arrangement. The fluorescence signal is collected by a 5 cm diam f/1 CaF_2 lens and focussed onto a 5 mm slit positioned directly in front of the phototube, resulting in a factor of 30 improvement in signal to noise. The afterglow background is also reduced by chemical quenching by addition of trace gases and by the use of filters in the photomultiplier housing; short wavelength cutoff filters are effectively used in combination with bandpass filters. Nevertheless, the ultimate signal-to-noise is still limited by the continuous afterglow background light.

A boxcar signal averager provides a variable width, variable position window for gated collection of fluorescence. The boxcar is triggered by the Q-switch of the Nd:YAG laser, the gate is normally delayed by about one molecular radiative lifetime to minimize scattered light, and it is then opened for several lifetimes for signal acquisition. The current from the photomultiplier is transformed by the boxcar into a digitally held voltage which is a measurement of the average signal over the gate width. The laser power as measured by a thermopile is simultaneously monitored in the second channel of the boxcar. The fluorescence signal normalized for laser power is then directly taken as an output.

In a typical experiment, the reactant ion is generated in the ion source and reacts downstream with a neutral reagent to form vibrationally excited products just before the laser excitation port. The tunable dye laser induces a transition from specific vibrational and rotational levels of the products to a bound electronic state; the total visible or ultraviolet fluorescence from this state is monitored with the photomultiplier. The boxcar signal averager provides the gated detection of the fluorescence and normalization to the laser power while the dye laser wavelength is slowly scanned through a vibronic band of the species of interest. The resulting LIF excitation spectrum is recorded by coupling the boxcar output with a strip chart recorder or with a multichannel analyzer connected to a minicomputer.

A laser-induced fluorescence spectrum for $OH[A\ ^2\Sigma^+(v'=1) - X\ ^2\Pi\ (v''=0)]$ formed in the reaction of O^- with HF is shown in Fig. 5. The excellent signal-to-noise possible with LIF is clearly evident; signal levels of 2000 counts/sec are easily obtained with total background signals of only a few counts/sec. Typical scan rates of 0.05 nm/min require reasonably short times (about 15 min) for data acquisition, and therefore stability of experimental parameters is excellent.

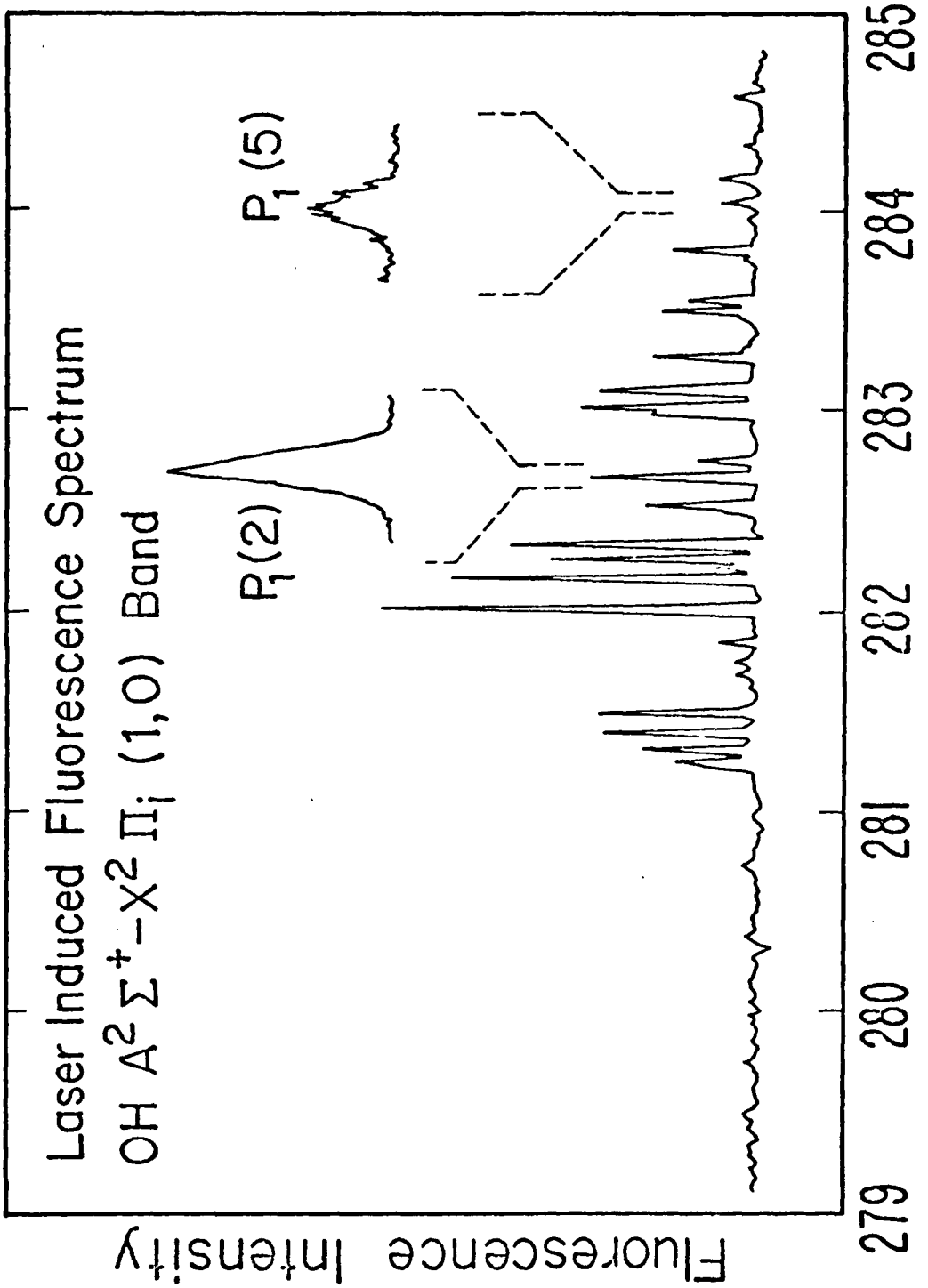

Fig. 5. Laser-induced fluorescence spectrum of the (1,0) band of OH ($A\ ^2\Sigma^+ - X\ ^2\Pi i$) produced in the reaction $O^- + HF \rightarrow OH(v=0,1) + F^-$. The well-isolated lines $P_1(2)$ and $P_1(5)$ are shown for a typical slow scan. The areas of these lines are used to determine the population in the v"=0 state.

The peak or integrated fluorescence intensities of single lines are corrected for relative transition probabilities, the filter transmission curves, and the photomultiplier quantum efficiency as a function of wavelength. Nonradiative loss processes of the excited state must also be considered. In particular, vibrational deactivation of the upper state can be a serious problem even for collisions with helium (Miller and Bondybey, 1977; Katayama, et al., 1980). This problem is conveniently circumvented by selecting transitions which terminate in the same upper state; in this way, vibrational and rotational relaxation processes and radiative rates are identical, independent of the initial vibrational level probed.

As in the infrared chemiluminescence experiments, a variety of checks are carried out to insure that the detected products arise from the ion-molecule reaction of interest and that the measured vibrational populations are unrelaxed. The experimental tests are very similar with one exception: ion modulation with a shutter is not necessary in the LIF experiment due to the high spectral selectivity and the pulsed nature of the detection scheme. While the correlation of the detected ionic species, N_2^+ and CO^+, with ionic reactants is straightforward, careful checks on the origin of OH are necessary to confirm its formation by the ion-molecule reaction. Therefore, background OH signals are measured by holding the tungsten mesh at a repulsive potential, thereby blocking all ions. The data analysis assumes that saturation of a transition by the laser does not occur. The absence of saturation is confirmed experimentally by demonstrating that the fluorescence signal scales directly with laser power up to about 1 mJ/cm^2. Extraction of nascent populations from experiments carried out in the saturated regime is more complicated, but saturation conditions are used in the single collision apparatus to increase the signal-to-noise ratio.

2. Results

a. Proton transfer reactions

Proton transfer reactions,

$$Y^- + HX \rightarrow HY + X^- \quad , \qquad (1)$$

are among the simplest and most studied of ion-molecule processes. The rate constants and exothermicities of several of these reactions are collected together in Table I. Most of the proton abstraction processes described here occur adiabatically on a single potential energy surface, a fact which greatly simplifies the interpretative tasks. All reagents and products are closed shell species whose first excited electronic states are high in energy so that at thermal energies surface hopping trajectories are expected to be unimportant (Preston and Tully, 1971; Krenos, et al., 1974).

In light of the enormous amount of research on the dynamics of simple, neutral reactive encounters, Y + HX → HY + X (Kuntz, 1976), it is illuminating to compare the vibrational state distributions for corresponding neutral and ion reactions. The bottom of Table I provides data for the neutral reactions. It should be noted that the halogen atom reactions sometimes involve several interacting electronic states which lead to a number of coupled potential surfaces. Another important difference between neutral and ion reactions is the intermolecular potential. The potential between neutrals is only weakly attractive and generally features a barrier which must be surmounted for reaction to take place. In contrast, ion-molecule reactions feature potentials dominated by the attractive ion-dipole and ion-induced dipole terms and, consequently, pass through potential minima. Figure 6 is a sketch of the potential energy curves for collinear collisions of F with HCℓ and F^- with HCℓ. In both cases, the product HF can be excited up to v=3. As indicated in Table I,

Table I.

Exothermicities, rate constants, and product vibrational populations for several proton transfer and hydrogen atom transfer reactions.

Proton transfer reactions

Ion reaction	ΔH(eV)	$k(cm^3\ s^{-1})$[a]	N_0[b]	N_1	N_2	N_3	N_4	N_5	N_6	$\langle f_v \rangle$	Reference
$Cl^- + HBr \rightarrow HCl + Br^-$	-0.43	7.5(-10)	(0.60)	0.40						0.30	c
$Cl^- + HI \rightarrow HCl + I^-$	-0.83	6.3(-10)	(0.33)	0.36	0.31					0.46	c
$F^- + HCl \rightarrow HF + Cl^-$	-1.65	1.6 (-9)	(0.37)	0.29	0.21	0.13				0.31	d
$F^- + HBr \rightarrow HF + Br^-$	-2.08	1.2 (-9)	(0.24)	0.21	0.21	0.18	0.16			0.40	d
$F^- + HI \rightarrow HF + I^-$	-2.48	1.0 (-9)	(0.15)	0.17	0.19	0.19	0.17	0.13		0.45	d
$O^- + HF \rightarrow OH + F^-$	-0.46	~5 (-10)	0.82	0.18						0.15	e
$CN^- + HCl \rightarrow HCN + Cl^-$	-0.77	3.0 (-9)	---	0.89	0.11						f
$CN^- + HBr \rightarrow HCN + Br^-$	-1.19	2.4 (-9)	---	0.51	0.44	0.05					f
$CN^- + HI \rightarrow HCN + I^-$	-1.59	1.3 (-9)	---	0.21	0.47	0.11	0.02	(HNC,	0.19)		f

Hydrogen atom transfer reactions

Neutral reaction	ΔH(eV)	$k(cm^3\ s^{-1})$[a]	N_0[b]	N_1	N_2	N_3	N_4	N_5	N_6	$\langle f_v \rangle$	Reference
$Cl + HBr \rightarrow HCl + Br$	-0.68	8.4(-12)	(0.58)	0.38	0.04					0.22	c
$Cl + HI \rightarrow HCl + I$	-1.38	1.5(-10)	(0)	0.10	0.15	0.43	0.32			0.71	g
$F + HCl \rightarrow HF + Cl$	-1.44	8.1(-12)	(0.07)	0.23	0.60	0.10				0.51	h
$F + HBr \rightarrow HF + Br$	-2.11	4.5(-11)	(0.04)	0.13	0.16	0.29	0.38			0.59	h
$F + HI \rightarrow HF + I$	-2.82	4.1(-11)	(0.06)	0.10	0.11	0.13	0.16	0.20	0.24	0.59	h
$O + HF \rightarrow OH + F$	1.48	---									
$CN + HCl \rightarrow HCN + Cl$	-0.97	3.7(-14)									i
$CN + HBr \rightarrow HCN + Br$	-1.65	3.7(-13)									i
$CN + HI \rightarrow HCN + I$	-2.36	7.6(-12)									i

Notes for Table I

[a] The tabulated rate constants abbreviate the exponent.
[b] Where available the values for N_v are given. These are the best estimates of the v=0 population based on an extrapolation of a surprisal analysis (Levine, 1978). The N_v value for the $O^- + HF$ reaction is determined absolutely. The tabulated N_v values are normalized so that they sum to unity.
[c] Zwier, et al. (1978).
[d] Weisshaar, et al. (1981).
[e] Hamilton, et al. (1982).
[f] Maricq, et al. (1981), the N_v's describe the ν_3 C-H stretch mode of HCN and the N-H stretch of HNC.
[g] Maylotte, et al. (1982).
[h] Cold wall corrected relaxation data of Tamagake, et al. (1980).
[i] Roden (1975).

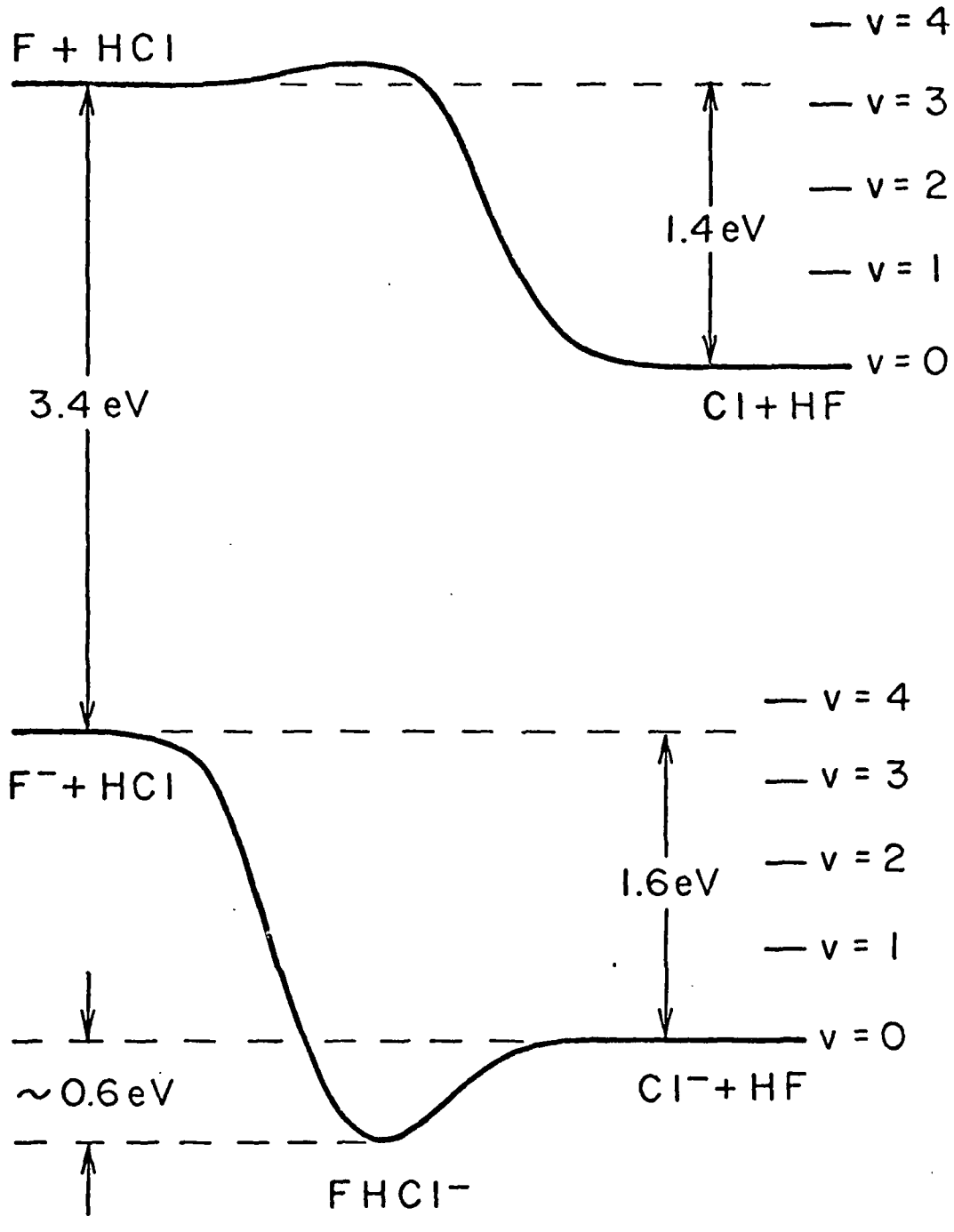

Fig. 6. Schematic drawing showing the difference between typical potential energy surfaces for a neutral, F + HCℓ → HF(v=0-3) + Cℓ, and an ion, F^- + HCℓ → HF(v=0-3) + $Cℓ^-$, reaction [from Weisshaar, et al. (1981)].

the exothermicities of the ion reactions are comparable to their neutral analogs but the rate constants are roughly 2 or 3 orders of magnitude larger. The fast rates of ion-molecule reactions are generally attributed to the presence of the large, attractive well. In general, both the ion and neutral reactions have a tendency to dispose of a large fraction of the exothermicity into product vibration.

The details of the reaction dynamics of several proton transfer reactions have been studied by infrared chemiluminescence (Zwier et al., 1980a; Weisshaar et al., 1981):

$$Cl^- + HBr, HI \rightarrow HCl(v) + Br^-, I^- \qquad (2)$$

$$F^- + HCl, HBr, HI \rightarrow HF(v) + Cl^-, Br^-, I^- \qquad (3)$$

For the reaction of Cl^- with HBr, there is only enough energy (0.43 eV) to produce HCl(v=0,1). Infrared emission from HCl(v=1) at 3.47 μm is observed but there are no direct means of monitoring the population born in v=0. In the reaction of Cl^- with HI, production of HCl(v=0,1,2) is possible and the emission of HCl(v=1) at 3.47 μm is separated from that of HCl(v=2) at 3.60 μm by use of an HCl gas filter. From these measured chemiluminescence intensities and the known Einstein coefficients, the relative populations, corrected for radiative cascading and collisonal relaxation, are found to be v=2/v=1 = 0.85. Comparison of the Cl^- + HBr and HI emission intensities and further comparison of Cl^- + HI with the Cl^- + H associative detachment reaction allows approximate populations in v=0 to be assigned (Zwier, et al., 1980a). This comparison is based on the fact that the associative detachment reaction forms very little v=0 product. The numbers in Table I are based on the surprisal analysis for Cl^- + HI and they differ only slightly from the experimental comparison.

The reactions of F^- with HCℓ, HBr, and HI provide a much broader dynamical range; excitation of HF up to v=5 is possible with HI. Figure 3 shows the emission spectrum obtained from the product HF(v) formed in each case. These spectra are composed of multiple features which arise from the superposition of the P and R branches of the anharmonic bands. Figure 3 shows that successively higher vibrational bands are produced on going through the series F^- + HCℓ, HBr, and HI. Indeed the highest vibrational level observed in emission corresponds in all cases to the highest vibrational state allowed by the exothermicity. About 40 to 60 points define each spectrum in Fig. 3 and these spectra are inverted as described earlier to obtain vibrational populations. In this calculation, a room temperature Boltzmann distribution is assumed, and the positions, line strengths, and spectral resolution are specified. The average results of the relative vibrational populations after correction for radiative cascading are displayed in Table I (Weisshaar, et al., 1981).

The relative populations can be used to generate the complete product distribution if the v=0 population is known. These populations are estimated from a surprisal analysis (Levine, 1978) and are included in Table I in parentheses. Therefore one can approximately determine $\langle f_v \rangle$, the average fraction of the available energy deposited in product vibration. As evident from Table I, these fractions are substantial, ranging from 0.30 to 0.46 for the proton transfer reactions of $Cℓ^-$ and F^-.

Comparison of the ion and neutral populations in Table I shows many similarities. Both types of reactions lead to highly vibrationally excited HY product molecules but with the neutral reactions producing distinctly higher excitation. It is important to note that the kinematic effects for both ion and neutral reactions may be similar since both have identical mass combinations

of two heavy particles (H and H') and one light particle (L): HL + H' → H + LH'. In both cases the mass-weighted coordinate system (which diagonalizes the kinetic energy) is sharply skewed (Kuntz, 1976). This means that the entrance and exit valleys are rotated from each other by about 15°. Although the kinematics for the ion and neutral are similar, the detailed mechanisms of their interactions are expected to be very different. The possible presence of a long-lived intermediate in the ion reaction may allow for extensive redistribution of vibrational energy relative to the neutral process. The similarity of vibrational populations for ion and neutral reactions suggests that these simple proton transfer reactions, $Y^- + HX$, proceed through direct collisions with their dynamics being dictated largely by the kinematics rather than by the shape of the intermolecular potential. However, the lower f_v in most cases for the ion reactions suggests that the long range attractive forces do influence the final vibrational distribution to be somewhat more statistical.

A more complicated proton transfer process is the reaction:

$$O^- + HF \rightarrow OH(v=0,1) + F^- \qquad (4)$$

The corresponding neutral reaction is endothermic by 1.48 eV and does not occur at room temperature. In this case LIF is used to detect the product OH molecules; a typical fluorescence spectrum is shown in Fig. 5 (Hamilton et al., 1982). The LIF detection allows direct measurement of the populations of both vibrational states and no surprisal analysis is necessary. The absolute vibrational populations of OH products from this reaction are $N_0 = 0.82$ and $N_1 = 0.18$. The observed fraction in v=1 is significantly greater than would be expected by a statistical "prior" distribution (0.07) (Levine, 1978) even though the available energy is barely able to populate the v=1 state. A detailed interpretation of this reaction may be complicated by the multiple

states of $O^-(^2P_{3/2}$ and $^2P_{1/2})$ and $OH(^2\Pi_{3/2}$ and $^2\Pi_{1/2})$. The two spin orbit states of O^- are split by only 22 meV (Hotop and Lineberger, 1975) so that a mixture of reactant states is present in the flowing afterglow. However, the reactivity and detailed dynamics of these states may differ; for example, Tully (1974) finds a substantial difference in reactivity between the two fine structure states in the reaction of $F(^2P_{3/2}$ and $^2P_{1/2})$ with H_2. The splitting between the two spin-orbit states of OH is 16 meV (Evenson et al. 1970), the numerous collisions with helium preclude detection of any preferential excitation in the $^2\Pi_{3/2}$ and $^2\Pi_{1/2}$ product states of OH.

The reactions discussed so far have all been those of an atomic ion with a diatomic molecule to produce a vibrationally excited hydrogen halide. We next consider the reactions of CN^- with HX to produce vibrationally excited HCN (Maricq et al., 1981).

$$CN^- + HCl, HBr, HI \rightarrow HCN(v) + Cl^-, Br^-, I^- \qquad (5)$$

The study of IR emission from a triatomic molecule is considerably more difficult than from a diatomic species. It is now necessary to distinguish chemiluminescence from the C≡N stretch (ν_1), a doubly degenerate H-C≡N bend (ν_2), and the C-H stretch (ν_3). With so many modes, the spectroscopy becomes more complicated and the separation and assignment of emission lines becomes more difficult. Worse yet, the energy may scramble via intramolecular pathways so that the resulting emission bears little resemblance to the initial product state distribution. In an extreme case, the internal energy may rapidly leak out by collisional deactivation in the flow tube of a low frequency vibrational mode resulting in no emission at all.

Because of the favorable spectroscopic features (Allen, et al., 1956) and relaxation rates of HCN (Hariri, et al., 1976; Petersen and Smith, 1979;

Arnold, et al., 1980), it is possible to extract the relative populations in the v_3 mode produced by the reactions CN^- with HCℓ, HBr, and HI. These are summarized in Table I; no dynamical information is available for the corresponding CN reactions (Roden, 1975). Since population inversions are observed, it is apparent that the excess vibrational energy does not become completely scrambled among the available vibrational modes as the reactants pass through the deep potential well separating reactants and products. Unfortunately, very little can be said about the energy distribution in other modes except that a considerable number of bending quanta must be excited (v_2).

A second important and unexpected result of these studies is the detection of HNC, produced in the reaction of CN^- with HI. In fact, HNC represents roughly 20% of the excited products detected in this reaction. Hydroisocyanic acid, HNC, is identifiable by its characteristic N-H stretch at 2.74 μm. Figure 7 shows the results of a point-by-point scan of the Ge:Cu detector equipped with the circular variable filter through the high frequency N-H stretch region for HNC resulting from the CN^- + HI reaction. This is a nice example of the ability of the infrared method to sense a fragile reaction product not easily detected in any other way.

The thermochemistry of HNC is of some interest, and from our data we can make some quantitative statements. The difference in enthalpy between HCN and HNC is the isomerization energy, ΔH_{iso}, and the height of the barrier to isomerization of HNC(v=0) to HCN is the isomerization barrier, ΔE_{iso}. By considering which CN^- reactions produce excited HNC, the enthalpy difference between the two species can be bracketed (Maricq et al., 1981)

$$1.14\ (\pm 0.11)\ \text{eV} > \Delta H_{iso} > 0.74\ (\pm 0.11)\ \text{eV} \quad .$$

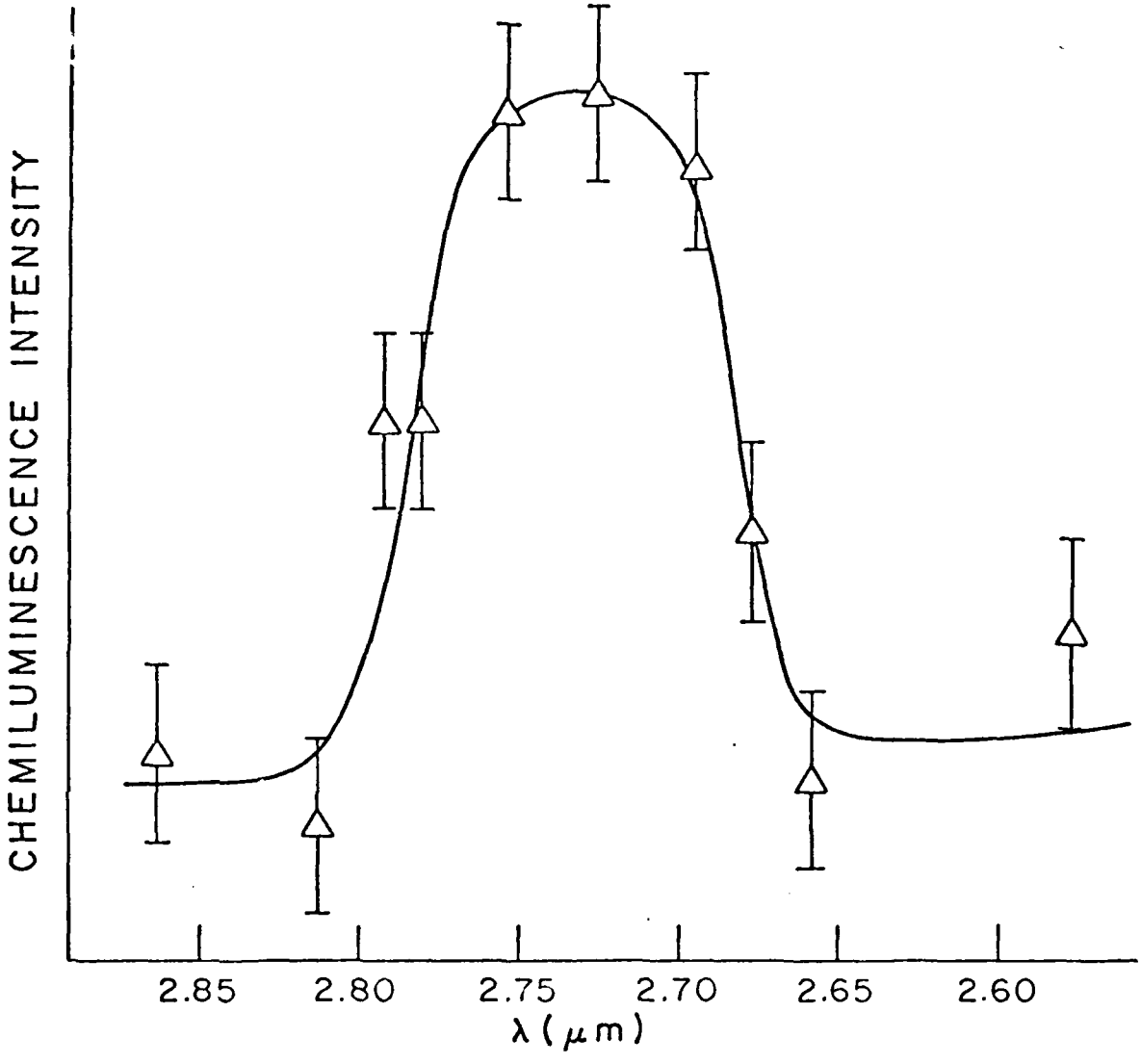

Fig. 7. Emission band from the NH stretch of HNC produced in the ion reaction of CN^- with HI. [From Maricq, et al. (1981)].

The uncertainty in the heats of reaction is traceable to the lack of precision in the heat of formation of HCN (Berkowitz, et al., 1968). Two recent experimental studies have independently measured ΔH_{iso} in a direct manner. A study of microwave absorption as a function of temperature reports a value of 0.44 ± 0.05 eV (Maki and Sams, 1981) while a deprotonation experiment in an ion cyclotron resonance spectrometer finds a value of 0.64 ± 0.09 eV (Pau and Hehre, 1982). Both our results and recent computational work (Redmon, et al., 1980; Dykstra and Secrest, 1981) favor the latter value. Using Pau and Hehre's value for ΔH_{iso} and the fact that none of the HCN(v) product of the CN^- + H reaction isomerizes to HNC, we can likewise bound the isomerization energy:

$$\Delta E_{iso} \geq 0.92\ (\pm 0.11)\ eV \quad .$$

This result is consistent with calculated theoretical barriers (Redmon, et al., 1980) of 1.3 eV.

b. Associative detachment reactions

Associative detachment reactions, $A^- + B \rightarrow AB(v,J) + e^-$, offer a novel opportunity to probe the transition of a negative ion potential energy surface into a neutral plus electron continuum. The flowing afterglow infrared method provides detailed information on these processes by investigation of state distributions in the neutral product molecule. There is tremendous interest in several processes which proceed through negative ion molecular states, including electron-scattering, dissociative attachment, and associative detachment (Shimamura and Matsuzawa, 1979). Thus far, there is no unifying theoretical description of these interrelated processes. Associative detachment is unique among these in that it samples the negative ion surface from long range. As the internuclear separation decreases, the neutral surface becomes unstable

with respect to autodetachment (for representative HF and HF^- surfaces, see Segal and Wolf, 1981). The vibration-rotation state distribution can provide a tremendous amount of information concerning the geometry and dynamics in the autodetachment region. There are numerous early discussions of the associative detachment process and of the important theoretical criteria (Fehsenfeld, 1975b; Herzenberg, 1967).

The infrared chemiluminescence/flowing afterglow technique has provided almost all of the recent data on vibrational product states in associative detachment reactions. The technique has been applied to five systems:

$$O^- + CO \rightarrow CO_2(v) + e^- \quad \text{(Bierbaum, } \underline{\text{et al.}}\text{, 1977)} \quad (6)$$

$$Cl^- + H \rightarrow HCl(v=0\text{-}2) + e^- \quad \text{(Zwier, } \underline{\text{et al.}}\text{, 1980b)} \quad (7)$$

$$CN^- + H \rightarrow HCN(v) + e^- \quad \text{(Maricq, } \underline{\text{et al.}}\text{, 1981)} \quad (8)$$

$$F^- + H \rightarrow HF(v=0\text{-}5) + e^- \quad \text{(Zwier, } \underline{\text{et al.}}\text{, 1981, Smith and Leone, 1982)} \quad (9)$$

$$F^- + D \rightarrow DF(v=0\text{-}7) + e^- \quad \text{(Smith and Leone, 1982)} \quad (10)$$

The O^- + CO reaction was the first ion-molecule reaction studied by infrared chemiluminescence in the flowing afterglow. Direct excitation of the product CO_2 antisymmetric stretch mode is observed. When a CO_2 gas filter cell is used to block the (001 → 000) emission, 30% of the fluorescence is transmitted, compared to about 10% which would be transmitted for a sample thermalized in the bending modes (0n0). This clearly indicates excitation in states higher than (001), which might also include excitation of other modes.

In the Cl^- + H reaction, the HCl vibrational distribution of v=2/v=1 is measured to be 0.6. This is less than the v=2/v=1 ratio of 0.85 for the Cl^- + HI reaction. However, comparison of the total emission intensity of these two

reactions, which have similar exothermicities, suggests that the formation of HCℓ(v=0) in the associative detachment reaction is zero or small. This is corroborated by the application of microscopic reversibility to data obtained by Allan and Wong (1981) on the reverse dissociative attachment process (Zwier, et al., 1980b). It is found that the associative detachment process strongly favors population of the highest vibrational states, and that the reverse, dissociative attachment cross sections are greatly enhanced by vibrational excitation. Figure 8 shows this propensity for high vibrational excitation even more dramatically for the F^- + H and D systems, which produce HF up to v=5 and DF up to v=7. There is a strong peaking of the vibrational excitation into the highest states accessible, a good indication that the electron detachment occurs at large separations in the initial approach of the F^- + H. The colliding atom and ion sample the highest vibrational states first and have a substantial probability of detaching into those high levels. Indeed, this physical description is supported by detailed theoretical calculations (Gauyacq, 1982; see also Zwier, et al., 1981). There is a significantly greater population of the lower vibrational states in the F^- + D case. This is attributed to a reduction in the probability for detachment at large internuclear separations, increasing the fraction of collisions which survive to closer separations and sample the lower vibrational levels (Smith and Leone, 1982). This result has not yet been satisfactorily explained by theory.

The release of the extremely light electron in the associative detachment process provides an interesting dynamical constraint due to conservation of energy and angular momentum. A substantial fraction of the orbital angular momentum of the incoming reactants is converted into rotational excitation of the neutral product molecule. For molecules with large rotational constants this has the effect of reducing the range of allowed impact parameters, and

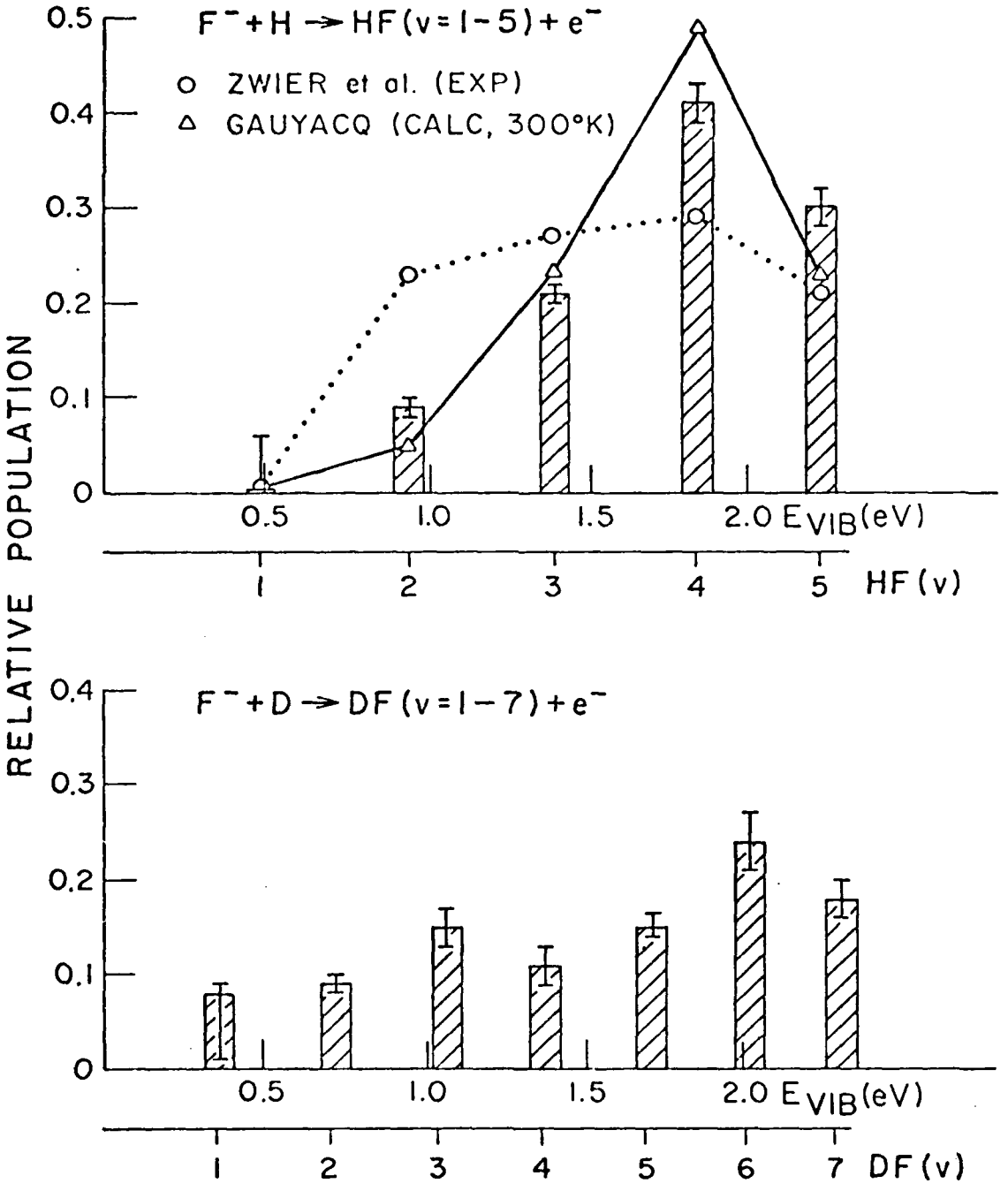

Fig. 8. Vibrational population distributions for the $F^- + H, D \rightarrow HF(v), DF(v) + e^-$ associative detachment reactions. Earlier data (O) of Zwier, et al. (1981) was found to be partially relaxed. Theoretical calculations (Δ) of Gauyacq (1982) show good agreement with the present results for HF.

hence the cross section, that can lead to the highest vibrational levels. This truncation of population in the highest vibrational states is readily apparent in Fig. 8. Simple model arguments can predict the near one-to-one mapping of impact parameter into rotational state (Zwier, et al., 1980b; Zwier, et al., 1981). In the more complete theoretical description when both vibrational and rotational states are taken into account, each vibrational state spans predominantly a small range of J values, and the cross sections into each successive vibrational level turn on and off at a certain J (Gauyacq, 1982). The production of high rotational states has recently been observed directly by carrying out the F^- + D reaction in a argon buffer gas, which is much less efficient than helium at rotational relaxation (Smith and Leone, 1982).

The population distribution in the C-H stretch of HCN is obtained for the CN^- + H associative detachment reaction and found to be v=1:v=2:v=3:v=4 ≡ 0.47:0.39:0.09:0.05 (Maricq, et al., 1981). Although there is substantial excitation, this distribution decreases with increasing vibrational level in contrast to the diatomic cases. This is attributed to the large number of vibrational states accessible in the polyatomic product, which reduces the probability of depositing all of the reaction exothermicity into the C-H mode. In the reaction of CN^- with HI, the HNC product is detected. Even though the CN^- + H reaction has a nearly identical exothermicity, the vibrationally excited HNC product is not observed in this case. It is conjectured that perhaps the approach of the H atom to the nitrogen end of the CN^- leads to a significant barrier in the potential surface, preventing the HNC^- species from ever reaching the autodetaching region (Maricq, et al., 1981).

c. Heavy Atom Transfer

With the flowing afterglow infrared chemiluminescence apparatus, the first quantitative measurements of infrared emission from an ionic product of an ion-molecule reaction have been made, specifically from vibrationally excited NO^+ formed in the reaction of N^+ with O_2 (Smith, et al., 1982):

$$N^+ + O_2 \rightarrow NO^+ + O \qquad \sim 45\% \qquad (11)$$

$$\rightarrow O_2^+ + N \qquad \sim 50\% \qquad (12)$$

$$\rightarrow O^+ + N_2 \qquad \sim 5\% \qquad (13)$$

The branching fractions have been summarized by Albritton, et al. (1979). This reaction serves as a major loss of N^+ in the earth's atmosphere. The reaction is rapid ($k = 6.1 \times 10^{-10}$ cm^3 s^{-1}, McFarland, et al., 1973) and the channel forming NO^+ is extremely exoergic, releasing 6.6 eV energy. The disposal of this large exothermicity is an intriguing question. Tully, et al., (1971) found low product translational energies in their crossed beam experiments. Albritton, et al. (1979) found less than 2% formation of the first electronically excited state, NO^+ ($a\ ^3\Sigma^+$), in flowing afterglow studies. Therefore vibrational excitation is highly probable and levels up to v=28 are energetically accessible. This would produce infrared emission between 4 and 7 μm, a region where there are unidentified emissions in the earth's atmosphere. With oxygen pressures where the $N^+ + O_2$ reaction goes to approximately 50% completion, infrared emission is observed between 4.1 and 5.2 μm, peaking near 4.5 μm (Fig. 9). There is no emission at longer wavelengths. If the oxygen pressure is increased tenfold an intense new emission feature appears, centered at 5.7 μm and spanning 5.2-6.4 μm; the original emission remains essentially unchanged.

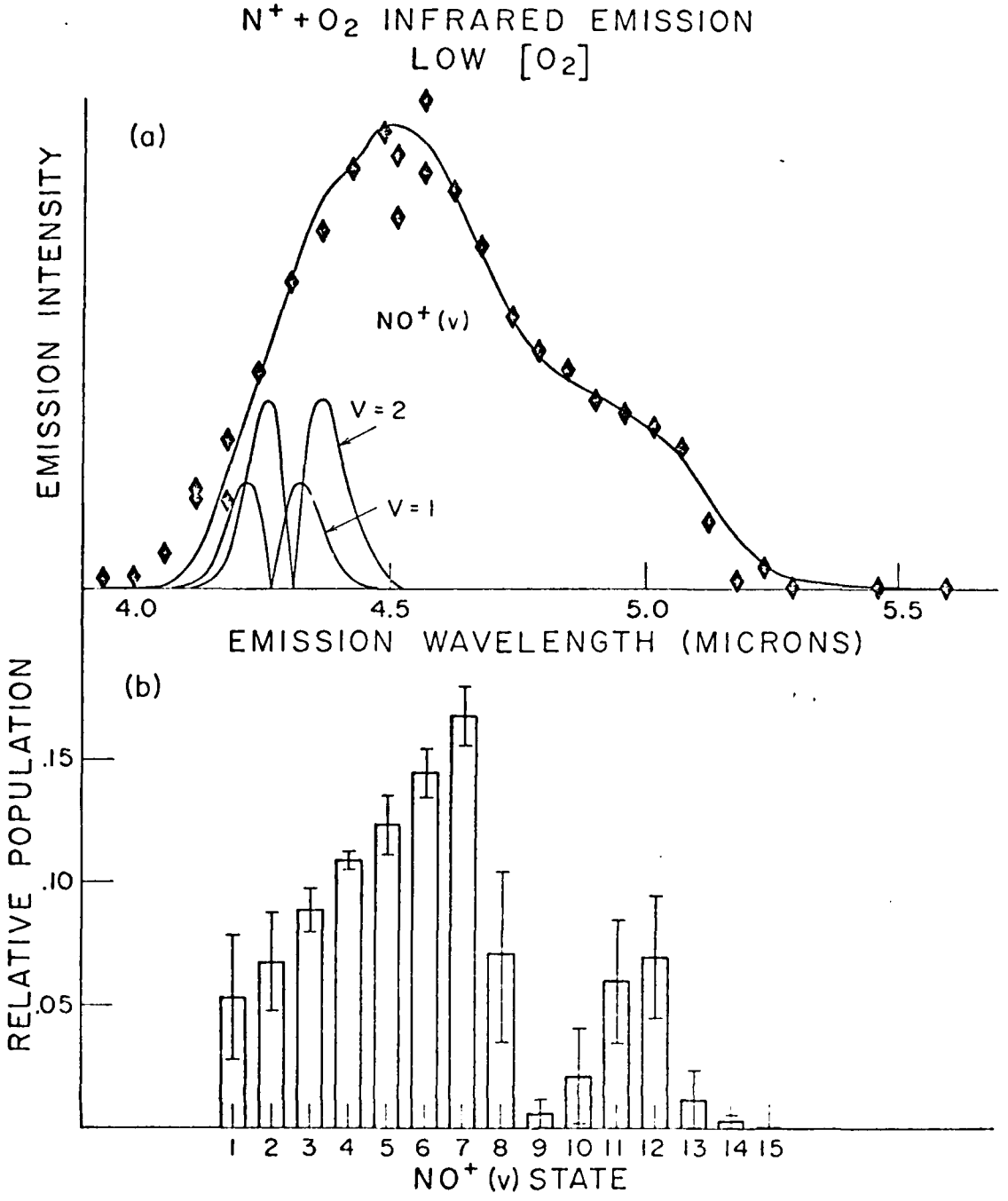

Fig. 9. (a) Infrared chemiluminescence spectrum of $NO^+(v)$ from the $N^+ + O_2 \rightarrow NO^+(v) + O$ reaction. The individual contributions from the v=2-1 and v=1-0 bands are shown underneath. The solid line is the best fit given by the bar graph populations (b).

These results suggest a more complex reaction scheme. The reactions of N^+ with O_2 are sufficiently exothermic that several electronically excited states of the product atoms are accessible:

		ΔH	
$N^+ + O_2$	$\rightarrow NO^+ + O(^3P)$	-6.6 eV	(14)
	$\rightarrow NO^+ + O(^1D)$	-4.6 eV	(15)
	$\rightarrow NO^+ + O(^1S)$	-2.4 eV	(16)
	$\rightarrow O_2^+ + N(^4S)$	-2.5 eV	(17)
	$\rightarrow O_2^+ + N(^2D)$	-0.1 eV	(18)

Although $NO^+(v=28)$ can be populated in the reaction forming the $O(^3P)$ product, only levels up to v=18 and v=8 are allowed for the $O(^1D)$ and $O(^1S)$ channels, respectively. Likewise, in addition to formation of O_2^+ and $N(^4S)$, there is a nearly energy resonant channel that can generate $N(^2D)$. $N(^2D)$ can undergo a well known reaction at the higher pressures of oxygen (Lin and Kaufman, 1971):

$$N(^2D) + O_2 \rightarrow NO(v) + O \qquad (19)$$

This reaction proceeds with a rate constant of 6×10^{-12} cm^3 s^{-1} and is sufficiently exothermic to populate $NO(v \leq 18)$, which appears to be the source of the additional emission. The corresponding reaction of $N(^4S)$ with O_2 would not occur under our experimental conditions ($k = 9 \times 10^{-17}$ cm^3 s^{-1}, Baulch, et al., 1973). Using radiative lifetimes for NO^+ (Werner and Rosmus, 1982) and for NO (Billingsley, 1976) we have carried out a computer fitting of the infrared data and obtain relative vibrational populations. Those for $NO^+(v)$ are shown in Fig. 9. The $NO^+(v)$ distribution is bimodal peaking at v=7 and 12,

indicating partitioning of the corresponding O atom product into at least two of the accessible states, ^3P, ^1D and ^1S. The absence of any population in levels greater than v=14 suggests that the $O(^3P)$ channel does not occur significantly. With the observation of low translational (Tully, et al., 1971) and low vibrational excitation, occurrence of the $O(^3P)$ pathway would require the unlikely channeling of about 3 eV into rotation. The rapid cutoff in emission near v=8 corresponds to the exothermicity of the product channel forming $O(^1S)$. The sum of $NO^+(v=1-8)$ and $NO^+(v=9-14)$ populations are in an approximate ratio of 5:1. While it is tempting to assign these emissions to the $O(^1S)$ and $O(^1D)$ channels, other interpretations of the data are possible.

The longer wavelength emission which arises at high oxygen pressure is identified as arising from NO(v) formed by further reaction of the $N(^2D)$ product. Our best fit population for NO(v) is in excellent agreement with the experimental results of Kennealy and co-workers (1978). Comparison of the relative intensities of NO^+ and NO emission suggest that the $N(^2D)$ is the major charge transfer product channel, representing 0.7 ± 0.2 of the total charge transfer process. The formation of NO(v) therefore serves as a convenient probe of otherwise "dark" ion-molecule reaction channels. These results present an interesting contrast with those of HCℓ and HF where very high vibrational excitation is observed. When electronically excited atomic products are possible, it appears that these channels are preferred, leaving less energy for vibrational excitation of the diatomic product. Nevertheless, a substantial amount of the available energy is emitted as vibrational chemiluminescence.

Vibrational relaxation rates of $NO^+(v)$ with NO and with N_2 have been measured by Bien (1978) and are relatively slow. The fact that our $NO^+(v)$ distribution does not change significantly for a wide range of oxygen pressures suggests that relaxation by O_2 may be inefficient.

d. Rotationally Resolved Charge Transfer

In the flowing afterglow, product molecules typically suffer thousands of collisions with the helium buffer gas before detection. This has the unfortunate consequence that rotational state distributions in all but a few cases are completely thermalized. In many ion-molecule reactions the rotational state populations will provide an important determinaton of the dynamical characteristics. A new apparatus has been developed which preserves the advantageous features of the high ion density and thermalized ions available in the flowing afterglow, but in which the ion reaction is carried out in a low pressure chamber under nearly single collision conditions (Guyer, et al., 1982).

Figure 10 shows the source and interaction region of this apparatus. A flowing afterglow source is coupled to a low pressure chamber by a large diameter (3-5 mm) orifice. With roughly 130 Pa pressure behind the nozzle orifice, the helium-entrained ions form a novel, low Mach number, free jet expansion into the high vacuum region. Densities of thermalized ions of approximately 10^6 cm^{-3} are achieved in the reaction zone with a background pressure of 0.04 Pa. Only about 10% of the ions undergo reaction with the crossed spray of reagent molecules, so that nearly single collision conditions are achieved. The product state distribution is probed by laser-induced fluorescence. In order to obtain sufficient signal-to-noise, the pulsed excitation laser is operated in the saturating regime. The signal count rates are typically one photon per laser pulse on a single line in the laser-induced fluorescence spectrum, with background count rates of 0.1 per laser pulse.

The nozzle expansion produces ions with well-characterized translational and internal energies. Laser-induced fluorescence measurements of diatomic ions such as CO^+ delivered through the expansion show rotational distributions

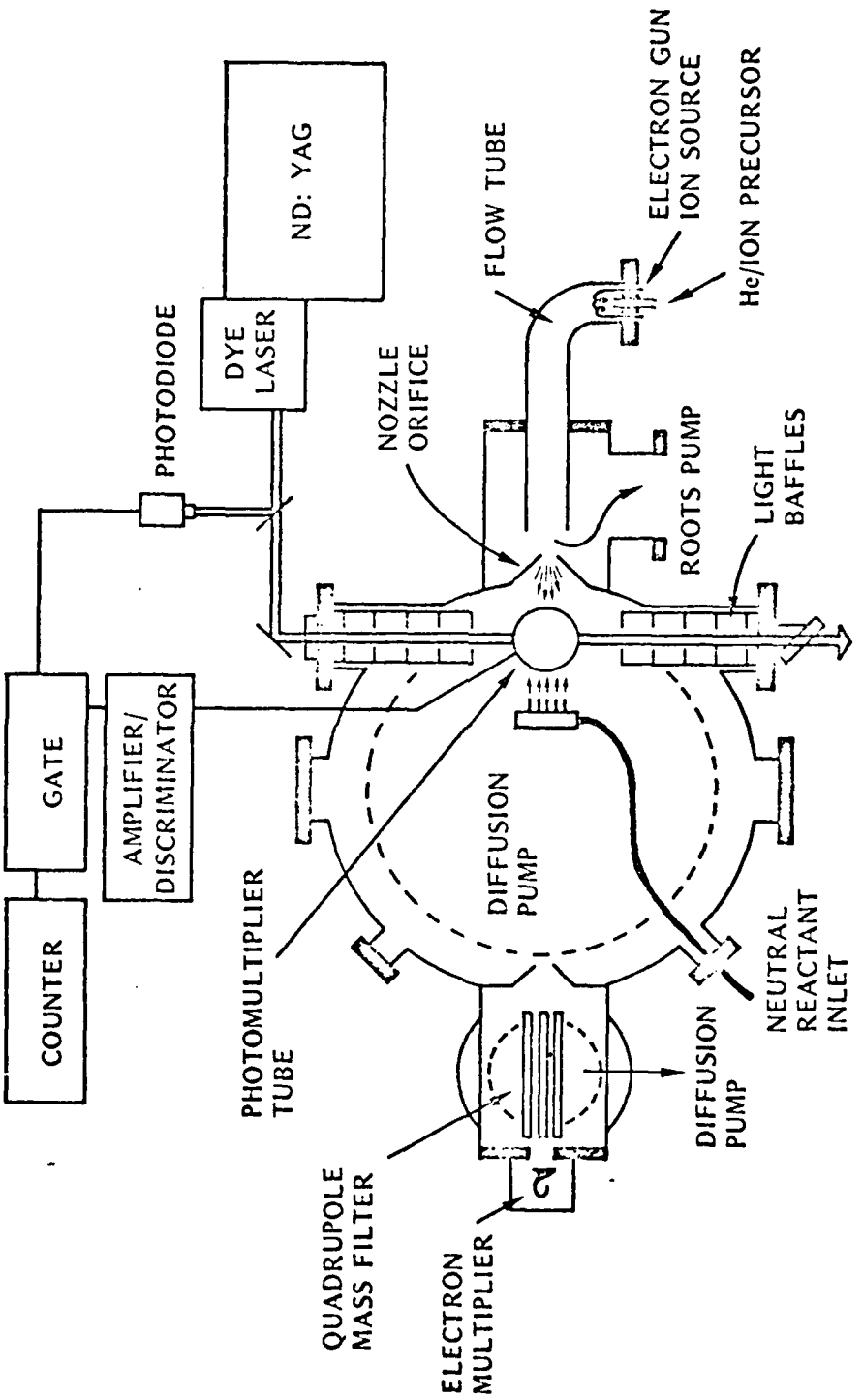

Fig. 10. Schematic drawing of the apparatus used to study thermal energy ion-molecule reactions under single collision conditions.

that are typically non-Boltzmann. The low rotational states are about 70 K and the higher states about 130 K. This can be explained by the varying rates of rotational relaxation, which decrease with increasing energy spacing between rotational levels. The translational energy is typically 0.1 eV, only slightly above thermal.

Results have been obtained for the charge transfer reaction

$$N^+ + CO \rightarrow N + CO^+ \qquad (20)$$

which is sufficiently exothermic to populate up to $CO^+(v=2)$. Population is predominantly observed in the v=0 state of CO^+, with only a small amount in the resonant state v=2 (Guyer, et al., 1982). A portion of the LIF spectrum from CO^+ (v=0) produced in the reaction is shown in Fig. 11. The rotational state distribution in v=0 fits approximately a Boltzmann distribution at a temperature of 430 K. Therefore the reaction energy is almost completely released into translation. A physical picture of this reaction is one in which the electron transfer occurs at large internuclear distances, delivering a near-Franck-Condon population in the CO^+ products. Such a process is called an electron jump with momentum transfer (Marx, 1978). It is characterized by an electron transfer at a distance where the difference potential between the N^+ + CO system and the CO^+ + N system goes to zero. For N^+ + CO this crossing occurs at long range. The low degree of rotational excitation suggests that the N + CO^+ products do not exert much torque on the CO^+ rotor in the exit channel. This may be the case if, once the elecron is transferred, the energy is released relatively slowly. This is consistent with the fact that the ion-induced forces are comparable in magnitude to the overall exothermicity. There are many other possibilities where the capability for rotationally-resolved product state distributions can be used to test important dynamical concepts in near-thermal energy ion-molecule reactions.

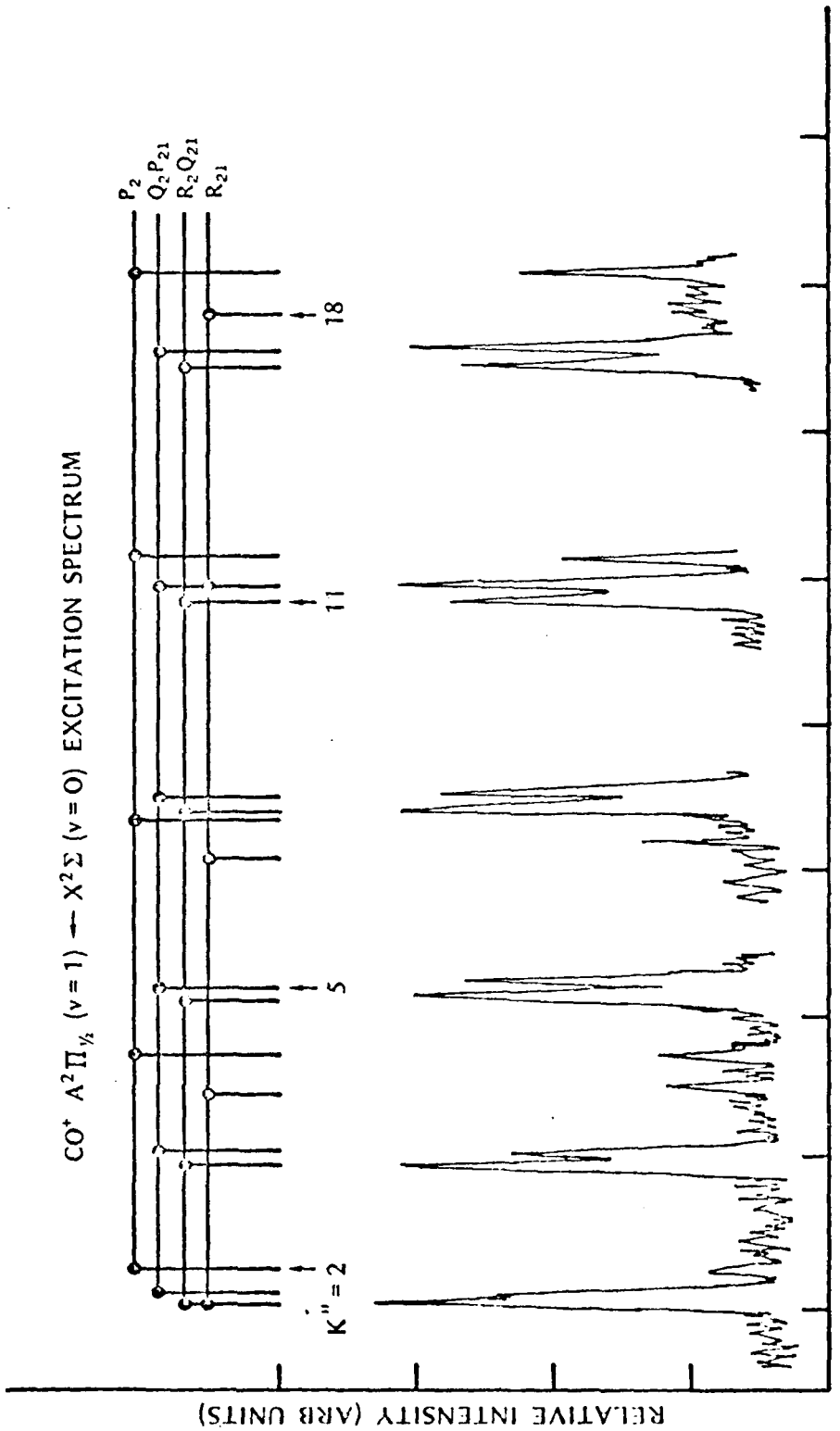

Fig. 11. Laser-induced fluorescence spectrum of a small portion of the rotational states in the $CO^+(A-X)$ system used to probe the rotational state populations in the X, v"=0 state produced by the $N^+ + CO$ charge transfer reaction.

e. Collisional Excitation and Relaxation of Ions

The flowing afterglow coupled with laser induced fluorescence allows studies of collisional energy transfer of ions. This is a challenging and important new area, for which little experimental data exist. The kinetic energy dependence of ion-molecule reaction rate constants and branching ratios have been addressed in drift tubes and flow drift systems, and the translational energy distribution of atomic ions in atomic buffer gases has been characterized. However, the extent of internal excitation of diatomic or polyatomic ions in a drift field is completely unknown. Dotan, et al. (1978) have observed a number of unusual changes in the reactivity of ions in a drift field which they attribute to vibrational excitation. In quadrupole ion trap studies, Mahan, et al., (1982) find that for charge transfer cross sections of $N_2^+(v)$, there is a strong dependence on vibrational excitation for reaction with N_2 and no measurable dependence for reactions with Ar.

Strikingly little information exists on energy transfer processes for ions even at thermal energy. Bien (1978) has measured relatively slow deactivation rates of $NO^+(v)$ by NO and N_2 and Howorka, et al. (1980) find essentially no relaxation of $N_2^+(v=1)$ by helium. There is evidence that symmetric charge transfer processes rapidly deactivate vibrationally excited ions (Mahan, et al., 1982). In preliminary studies we have found that relaxation of $CO^+(v=1)$ is rapid by both CO and N_2, occurring with a probability between 0.1 and 1.0 per collision (Hamilton, et al., 1982). Deactivation in both cases can occur by near resonant vibrational energy transfer, and with CO, charge transfer deactivation is also possible. Danon and Marx (1982) have also reported rapid vibrational relaxation of CO^+ in their LIF/ion trap studies of the reaction of Ar^+ with CO.

To study collisional excitation and relaxation of ions we have incorporated a drift section immediately before and throughout the region of laser

interrogation as shown in Fig. 12. This region is composed of about 40 thin cylindrical sections of flow tube, separated by mylar spacers and connected by precision resistors. In the region of LIF detection, a small opening is covered with wire mesh to allow collection of fluorescence by the photomultiplier. For these experiments the pulsed dye laser is introduced through a window in the end flange of the flow tube and directed along the flow tube axis. Therefore the baffle arms and laser ports in the region of laser probing are eliminated and field perturbations are minimized. With applied potentials of up to 5V/cm and helium buffer gas pressures of about 65 Pa, E/N values of up to 32 Td are obtained (1 Td = 10^{-17}V cm^2). The field is estimated to be 99% uniform to within 78% of the flow tube radius (Albritton, 1967). For proper operation of a drift tube, ionic species of only one polarity can be present. Efficient separation of positive and negative ions requires densities of 10^7 cm^{-3} or less; therefore, in comparison with other studies, these drift experiments are performed with considerably lower ion concentrations and reduced signal-to-noise.

The N_2^+ ion is an excellent candidate for the first drift studies due to its short radiative lifetime and straightforward spectroscopy (Engelking and Smith, 1975). Figure 13a shows a portion of the LIF spectrum for the B $^2\Sigma_u^+$(v'=0) - X $^2\Sigma_g^+$(v"=0) transition in N_2^+ in the absence of a drift field (Duncan, et al., 1982). A least squares analysis of the relative peak intensities in the R branch yields a rotational temperature of 289 K indicating a relaxed thermal Boltzmann distribution of ground state rotational levels. When a field of 30.9 Td is applied to N_2^+ in helium buffer gas, the LIF spectrum in Fig. 13b results. The maximum intensity has shifted from K"=6 to K"=10 and a rotational temperature of 666 K is obtained. Varying either the length of drift section before laser interrogation or the time delay between

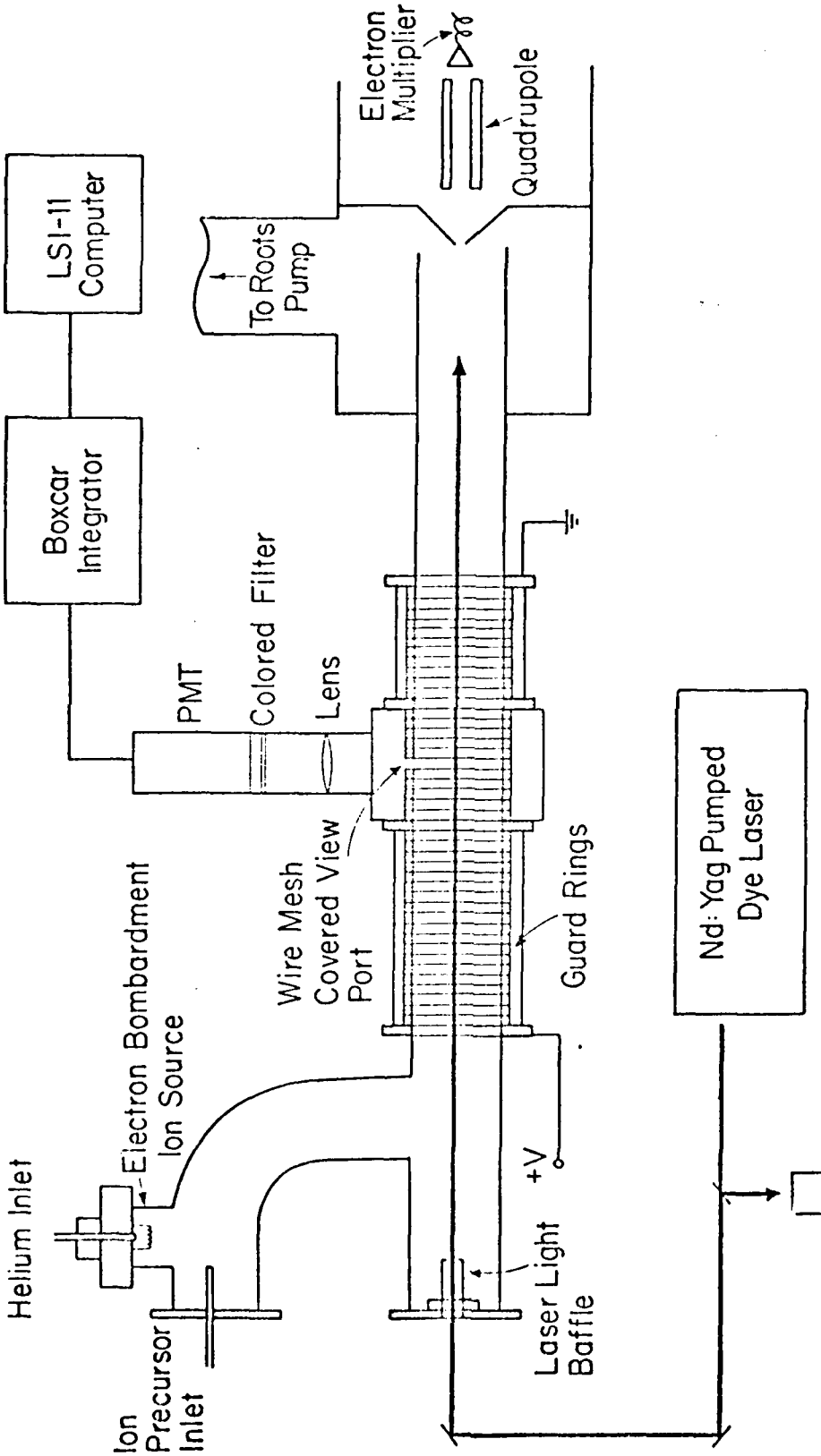

Fig. 12. Schematic drawing of the flow-drift tube used to study the internal excitation of ions in a drift field by laser-induced fluorescence.

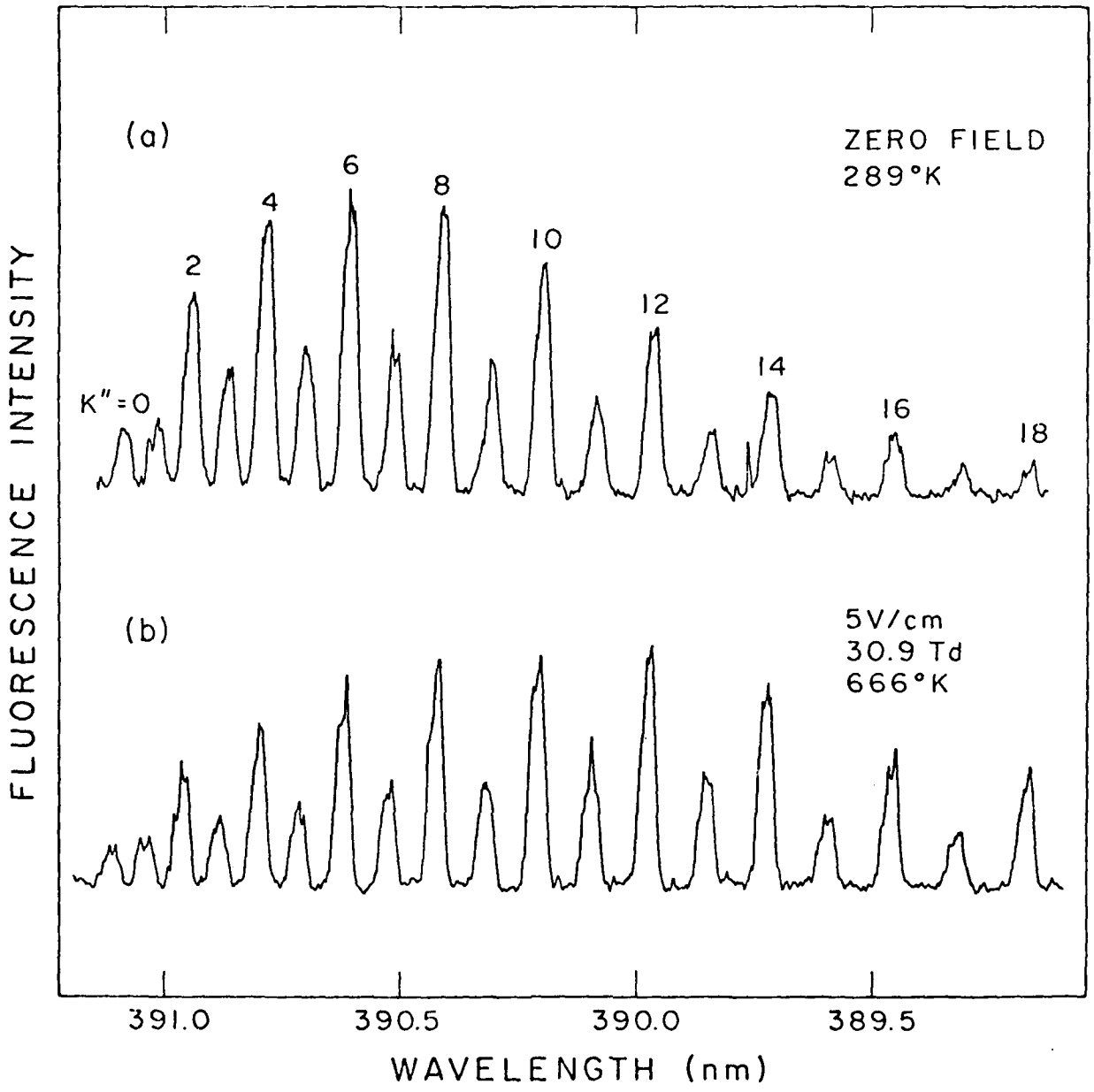

Fig. 13. Laser-induced fluorescence spectra of N_2^+ ($B\ ^2\Sigma_u$ - $X\ ^2\Sigma_g$) obtained by scanning the (0,0) transition while collecting the (0,1) emission through a bandpass filter. N_2^+ ions at (a) room temperature and (b) drifted at 30.9 Td in helium showing the effect of rotational heating. The spectra shown are not corrected for the transmission of the bandpass filter used.

application of the field and laser probing does not change the rotational temperature for a given E/N. This suggests that rotational excitation/relaxation processes in helium are very rapid, and equilibrium is achieved in less than ten collisions. Rapid translation-to-rotation energy transfer has also been reported by Mahan and O'Keefe (1982) in N_2^+-Ar collisions in an rf trap.

Viehland, et al. (1981) have developed a theoretical description of collisional excitation of ions in a drift field; in this treatment the internal temperature of an ion is simply given by the collision energy of the ions with the neutral buffer gas. Figure 14 plots the dependence of rotational temperature on field strength as predicted by theory and observed in the present experiments; the agreement is excellent.

3. Conclusion

Extension of the classical flowing afterglow technique to include infrared chemiluminescence and laser-induced fluorescence detection has provided a powerful new method for studying ion reaction dynamics. The diversity of processes outlined in the previous section is a testimony to the broad nature and versatility of this approach. Initial vibrational distributions for a variety of thermal energy ion-molecule reactions are determined for the first time; for some processes detailed rotational distributions are also obtained; collisional excitation and relaxation processes are studied both at thermal energy and as a function of kinetic energy.

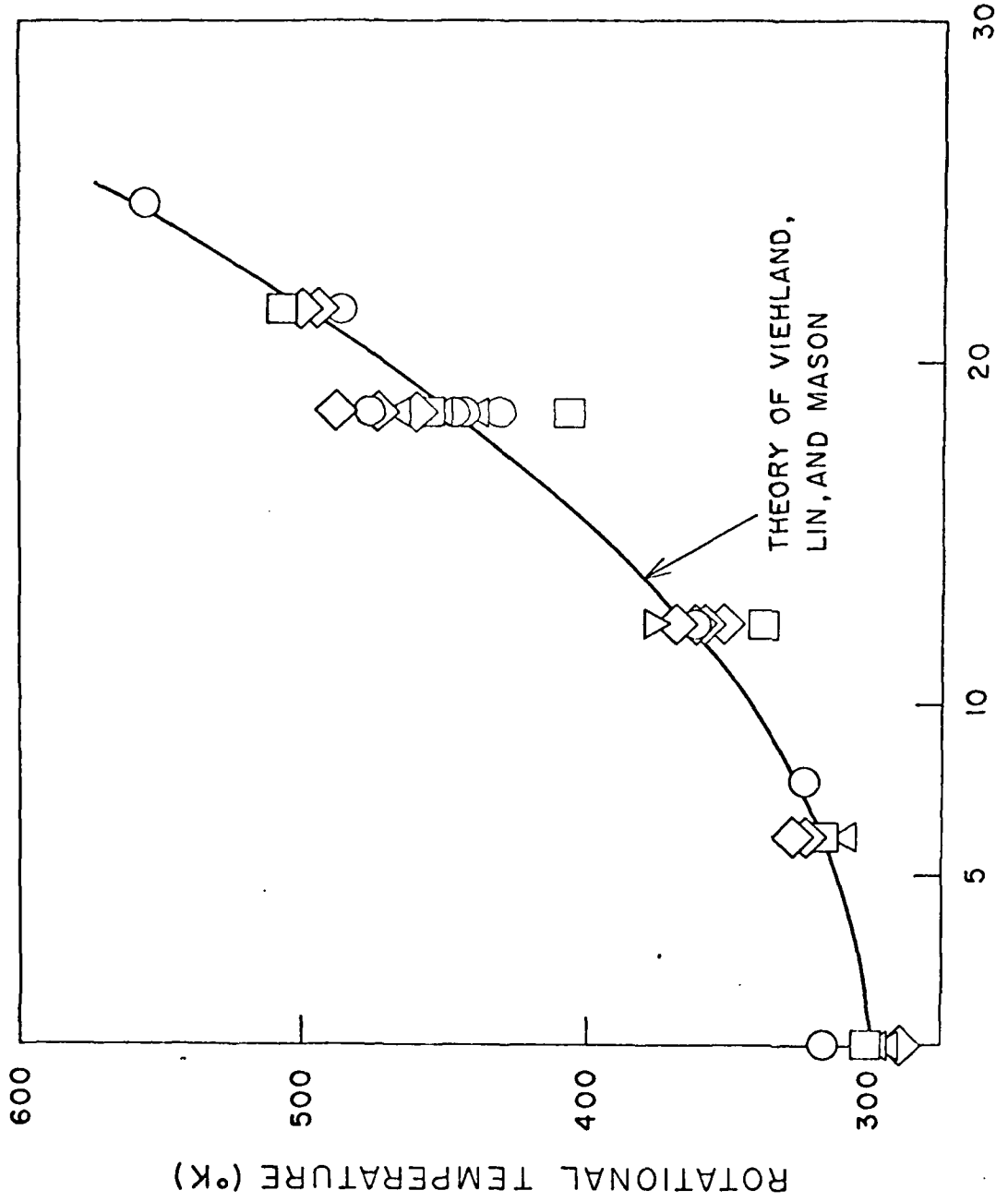

Fig. 14. Experimental results and theoretical predictions for the rotational temperature of N_2^+ drifted in helium versus E/N. The theory is from Viehland, et al. (1981).

4. References

Albritton, D. L. (1967). Ph.D. thesis, Georgia Institute of Technology, Atlanta, GA.

Albritton, D. L. (1978). At. Data and Nuclear Data Tables. 22, 1.

Albritton, D. L., Viggiano, A. A., Dotan, I., and Fehsenfeld, F. C. (1979). J. Chem. Phys. 71, 3295.

Allan, M., and Wong, S. F. (1981). J. Chem. Phys. 74, 1687.

Allen, Jr., H. C., Tidwell, E. D., and Plyler, E. K. (1956). J. Chem. Phys. 25, 302.

Arnold, G. S., Fernando, R. P., and Smith, I. W. M. (1980). J. Chem. Phys. 73, 2773.

Baulch, D. L., Drysdale, D. D., Horne, D. G. and Lloyd, A. C. (1973). "Evaluated Kinetic Data for High Temperature Reactions. II. Homogeneous Gas Phase Reactions of the H_2-N_2-O_2 System," Butterworths, London.

Berkowitz, J., Chupka, W. A., and Walter, T. A. (1968). J. Chem. Phys. 50, 1497.

Bien, F. (1978). J. Chem. Phys. 69, 2631.

Bierbaum, V. M., Ellison, G. B., Futrell, J. H., and Leone, S. R. (1977). J. Chem. Phys. 67, 2375.

Billingsley, F. P. II (1976). J. Mol. Spectry. 61, 53.

Danon, J., and Marx, R. (1982). Chem. Phys. 68, 255.

Dotan, I., Fehsenfeld, F. C., and Albritton, D. L. (1978). J. Chem. Phys. 68, 5665.

Duncan, M. A., Bierbaum, V. M., Ellison, G. B., and Leone, S. R. To be published.

Dykstra, C. E., and Secrest, D. (1981). J. Chem. Phys. 75, 3967.

Engelking, P. C., and Smith, A. L. (1975). Chem. Phys. Lett. 36, 21.

Evenson, K. M., Wells, J. S., and Radford, H. E. (1970). Phys. Rev. Lett. 25, 199.

Fehsenfeld, F. C. (1975a). Int. J. Mass Spectrom. Ion Physics 16, 151.

Fehsenfeld, F. C. (1975b). In "Interactions Between Ions and Molecules" (P. Ausloos, ed.), p. 387, Plenum, New York.

Ferguson, E. E., Fehsenfeld, F. C., and Schmeltekopf, A. L. (1969). Adv. At. Mol. Phys. 5, 1.

Gauyacq, J. P. (1982). J. Phys. B. To be published.

Guyer, D. R., HÜwel, L., and Leone, S. R. (1982). To be published.

Hamilton, C. E., Duncan, M. A., Zwier, T. S., Weisshaar, J. C., Ellison, G. B. Bierbaum, V. M., and Leone, S. R. (1982). To be published.

Hariri, A., Petersen, A. B., and Wittig, C. (1976). J. Chem. Phys. 65, 1872.

Herzenberg, A. (1967). Phys. Rev. 160, 80.

Hotop, H. and Lineberger, W. C. (1975). J. Phys. Chem. Ref. Data 4, 539.

Howorka, F., Albritton, D. L., and Fehsenfeld, F. C. (1980) Symp. on Atomic and Surface Physics, Maria Alm/SBG, February 10-16.

Katayama, D. H., Miller, T. A., and Bondybey, V. E. (1980). J. Chem. Phys. 72, 5469.

Kennealy, J. P., Del Greco, F. P., Caledonia, G. E., and Green, B. D. (1978). J. Chem. Phys. 69, 1574.

Krenos, J. R., Preston, R. K., Wolfgang, R., and Tully, J. C. (1974). J. Chem. Phys. 60, 1634.

Kuntz, P. J. (1976). In "Dynamics of Molecular Collisions, Part B," (W. H. Miller, ed.) p. 53, Plenum, New York.

Leone, S. R. (1982). J. Phys. Chem. Ref. Data. 11, .

Levine, R. D. (1978). Ann. Rev. Phys. Chem. 29, 59.

Lin, C., and Kaufman, F. (1971). J. Chem. Phys. 55, 3760.

Mahan, B. H., Martner, C., and O'Keefe, A. (1982). J. Chem. Phys. 76, 4433.

Mahan, B. H., and O'Keefe, A. (1982). Private communication.

Maki, A. G., and Sams, R. L. (1981). J. Chem. Phys. 75, 4178.

Maricq, M. M., Smith, M. A., Simpson, C. J. S. M., and Ellison, G. B. (1981). J. Chem. Phys. 74, 6154.

Marx, R. (1979). In "Kinetics of Ion-Molecule Reactions" (P. Ausloos, ed), p. 103, Plenum, New York.

Maylotte, D. H., Polanyi, J. C., and Woodall, K. B. (1972). J. Chem. Phys. 57, 1547.

McFarland, M., Albritton, D. L., Fehsenfeld, F. C., Ferguson, E. E., and Schmeltekopf, A. L. (1973). J. Chem. Phys. 59, 6610.

Miller, T. A., and Bondybey, V. E. (1977). Chem. Phys. Lett. 50, 275.

Pau, C. F., and Hehre, W. J. (1982). J. Phys. Chem. 86, 321.

Petersen, A. B., and Smith, I. W. M. (1979). J. Chem. Phys. 71, 3346.

Preston, R. K., and Tully, J. C. (1971). J. Chem. Phys. 54, 4297.

Redmon, L. T., Purvis, G. D. III, and Bartlett, R. J. (1980). J. Chem. Phys. 72, 986.

Roden, G. (1975). Ph.D. thesis, University of Göttingen.

Segal, G. A., and Wolf, K. (1981). J. Phys. B. 14, 2291.

Shimamura, I., and Matsuzawa, M. eds. (1979). "Symposium on Electron-Molecule Collisions." Univ. of Tokyo, Tokyo, Japan.

Smith, M. A., and Leone, S. R. (1982). To be published.

Smith, M. A., Bierbaum, V. M., and Leone, S. R. (1982). To be published.

Sung, J. P., and Setser, D. W. (1978). J. Chem. Phys. 69, 3868.

Tamagake, K., Setser, D. W., and Sung, J. P. (1980). J. Chem. Phys. 73, 2203.

Tully, J. C., Herman, Z., and Wolfgang, R. (1971). J. Chem. Phys. 54, 1730.

Tully, J. C. (1974). J. Chem. Phys. 60, 3042.

Viehland, L. A., Lin, S. L., and Mason, E. A. (1981). Chem. Phys. 54, 341.

Weisshaar, J. C., Zwier, T. S., and Leone, S. R. (1981). J. Chem. Phys. 75, 4873.

Werner, H.-J. and Rosmus, P. (1982). J. Mol. Spectry., submitted.

Zwier, T. S., Bierbaum, V. M., Ellison, G. B., and Leone, S. R. (1980a) J. Chem. Phys. 72, 5426.

Zwier, T. S., Maricq, M. M., Simpson, C. J. S. M., Bierbaum, V. M., Ellison, G. B., and Leone, S. R. (1980b). Phys. Rev. Lett. 44, 1050.

Zwier, T. S., Weisshaar, J. C., and Leone, S. R. (1981). J. Chem. Phys. 75, 4885.

C. Publications

1. V. M. Bierbaum, G.B. Ellison, J. H. Futrell and S. R. Leone, "Vibrational Chemiluminescence from Ion-Molecule Reactions: $O^- + CO \rightarrow CO_2^{\dagger} + e^-$," J. Chem. Phys. 67, 2375 (1977).

2. T. S. Zwier, M. M. Maricq, C.J.S.M. Simpson, V. M. Bierbaum, G. B. Ellison and S. R. Leone, "Direct Detection of the Product Vibrational-State Distribution in the Associative Detachment Reaction $Cl^- + H \rightarrow HCl(v) + e$," Phys. Rev. Lett. 44, 1050 (1980).

3. T. S. Zwier, V. M. Bierbaum, G.B. Ellison and S. R. Leone, "Vibrational Product State Distributions of Ion-Molecule Reactions by Infrared Chemiluminescence: $Cl^- + HBr, HI \rightarrow HCl(v) + Br^-, I^-$," J. Chem. Phys. 72, 5426 (1980).

4. M. M. Maricq, M. A. Smith, C.J.S.M. Simpson and G. B. Ellison, "Vibrational Product States from Reactions of CN^- with the Hydrogen Halides and Hydrogen Atoms," J. Chem. Phys. 74, 6154 (1981).

5. J. C. Weisshaar, T. S. Zwier and S. R. Leone, "Nascent Product Vibrational State Distributions of Ion-Molecule Reactions: The Proton Transfer Reactions $F^- + HX \rightarrow HF(v) + X^-$, X = Cl, Br, and I," J. Chem. Phys. 75, 4873 (1981).

6. T. S. Zwier, J. C. Weisshaar and S. R. Leone, "Nascent Product Vibrational State Distributions of Ion-Molecule Reactions: The $H + F^- \rightarrow HF(v) + e^-$ Associative Detachment Reaction," J. Chem. Phys. 75, 4885 (1981).

7. S. R. Leone, "Infrared Fluorescence: A Versatile Probe of State-Selected Chemical Dynamics," Acc. Chem. Res., in press.

8. M. A. Smith and S. R. Leone, "Product Vibrational State Distributions in Thermal Energy Associative Detachment Reactions: $F^- + H,D \rightarrow HF(v), DF(v) + e^-$," J. Chem. Phys., in press.

9. C. E. Hamilton, M. A. Duncan, T. S. Zwier, J. C. Weisshaar, G. B. Ellison, V. M. Bierbaum and S. R. Leone, "Product Vibrational Analysis of Ion-Molecule Reactions by Laser-Induced Fluorescence in a Flowing Afterglow: $O^- + HF \rightarrow OH(v=0,1) + F^-$," Chem. Phys. Lett., in press.

10. V. M. Bierbaum, G. B. Ellison and S. R. Leone, "Flowing Afterglow Studies of Ion Reaction Dynamics Using Infrared Chemiluminescence and Laser-Induced Fluorescence," Gas Phase Ion Chemistry, Vol. 3, "Ions and Light," M. T. Bowers, ed., in press.

11. M. A. Smith, V. M. Bierbaum and S. R. Leone, "Infrared Chemiluminescence from Vibrationally Excited NO^+: Product Branching in the $N^+ + O_2$ Ion-Molecule Reaction," Chem. Phys. Lett., in press.

12. M. A. Duncan, V. M. Bierbaum, G. B. Ellison and S. R. Leone, "Ion Collision Dynamics in a Drift Tube Studied with Laser-Induced Fluorescence: The Energy Dependent Rotational State Distribution of N_2^+," J. Chem. Phys., in preparation.

D. Professional Personnel Associated with the Research

Stephen R. Leone: Co-principal Investigator. Adjoint Professor, Department of Chemistry, University of Colorado. Staff Physicist, Quantum Physics Division, National Bureau of Standards.

G. Barney Ellison: Co-principal Investigator. Assistant Professor, Department of Chemistry, University of Colorado.

Veronica M. Bierbaum: Co-principal Investigator. Senior Research Associate, Special Member of the Graduate Faculty, Department of Chemistry, University of Colorado.

Timothy S. Zwier: Graduate Research Associate. Ph.D. Degree awarded August, 1981. Thesis: "Nascent Product Vibrational State Distributions in Gas-Phase Ion-Molecule Reactions."

James C. Weisshaar: Postdoctoral Research Associate, presently Assistant Professor, Department of Chemistry, University of Wisconsin.

M. Matti Maricq: Postdoctoral Research Associate, presently Assistant Professor, Department of Chemistry, Brown University.

C.J.S.M. Simpson: Visiting Scientist, Department of Chemistry, Oxford University, England.

Mark A. Smith: Graduate Research Associate. Ph.D. degree awarded August, 1982. Thesis: "Infrared Chemiluminescence and Neutral Products Identification Studies for the Determination of Ion-Molecule Reaction Dynamics."

Charles E. Hamilton: Graduate Research Associate, NSF Predoctoral Fellow.

Michael A. Duncan: NRC Postdoctoral Research Associate.

Zdenek Herman: Visiting Scientist, Czechoslovakian Academy of Science, Prague.

Jean H. Futrell: Visiting Scientist, Department of Chemistry, University of Utah.

E. Professional Interactions

V. M. Bierbaum - Seminars and Conferences

"Reaction Dynamics of Halide Ions," presented at the Western Regional Conference on Gaseous Ion Chemistry," January 9-11, 1981, Lake Arrowhead, California.

"Flowing Afterglow Studies of Ion-Molecule Chemistry and Dynamics," presented at the Symposium on Dynamics of Molecular Collisions," July 23-24, 1981, Williamsburg, Virginia.

"Vibrational State Dynamics of Gas Phase Ion-Molecule Reactions by Infrared Chemiluminescence and Laser Induced Fluorescence," presented at the Thirtieth Annual Conference on Mass Spectrometry and Allied Topics, June 6-11, 1982, Honolulu, Hawaii.

"Vibrational State Dynamics of Gas Phase Ion-Molecule Reactions by Infrared Chemiluminescence and Laser-Induced Fluorescence," presented at the International Symposium on Photochemistry and Chemical Reactions, June 14, 1982, Fukuoka, Japan.

"Gas Phase Chemistry of Organic Ions," January 19, 1979, Department of Chemistry, California Institute of Technology.

"Gas Phase Chemistry of Organic Ions," January 24, 1979, Department of Chemistry, University of California at Santa Barbara.

"Flowing Afterglow Studies of Ion-Molecule Chemistry and Dynamics," March 11, 1981, SRI International, Menlo Park, California.

"Gas Phase Studies of Ion-Molecule Chemistry and Dynamics," December 8, 1981, Department of Chemistry, Colorado State University.

"Gas Phase Studies of Ion-Molecule Chemistry and Dynamics," December 16, 1981, Department of Chemistry, Harvard University.

"Dynamics of Ion-Molecule Reactions by Infrared Chemiluminescence and Laser-Induced Fluorescence," June 22, 1982, Department of Chemistry, University of Tokyo.

S. R. Leone - Seminars and Conferences

"State-selected kinetics of laser excited species," Department of Chemistry Colloquium, Cornell University, Ithaca, New York, October 1979.

"Laser state-selected kinetics," Physical Chemistry Seminar, Northwestern University, Evanston, Illinois, November 1979.

"State-selected kinetics of laser excited species," Department of Chemistry Colloquium, Indiana University, Bloomington, December 1979.

"Infrared chemiluminescence studies of reactive dynamics," University of California, Berkeley, April 1980.

"Infrared chemiluminescence studies of reactive dynamics," University of Toronto, Toronto, Canada, May 1980.

"Electronic and ionic processes related to atomic and molecular lasers," Gordon Conference on Atomic and Molecular Interactions, Wolfeboro, New Hampshire, July 1980.

"Simple A+BC reaction dynamics with a negative ion flavour," Chemical Physics Seminar, Univ. of Colorado, Boulder, CO, Sept. 1980.

"Nascent product vibrational state distributions of simple ion-molecule reactions," Dept. of Chem., Colorado State Univ., Fort Collins, CO, Oct. 1980.

"Simple A+BC reaction dynamics with a negative ion twist," Dept. of Chem., Univ. of Denver, Denver, CO, Nov. 1980.

"Vibrational product state distributions of ion-molecule reactions," Symposium on "Chemistry and Dynamics of Ions and Molecules in the Gas Phase," 16th Midwest Regional American Chemical Society Meeting, Lincoln, Nebraska, Nov. 1980.

"Ion molecule reaction dynamics in the gas phase," The James Franck Institute, University of Chicago, February 1981.

"Dynamics of negative ion reactions," Department of Chemistry, Illinois Institute of Technology, February 1981.

"Dynamics of gaseous ion-molecule reactions," Max-Planck-Institut für Strömungsforschung, Gottingen, West Germany, March 1981.

"Laser studies of state-selected chemical dynamics," Chemistry Department Colloquium, University of Colorado, Boulder, CO, November 1981.

S. R. Leone - Seminars and Conferences (continued):

"Laser state-selected reaction dynamics," Department of Chemistry Colloquium, University of Arizona, Tucson, AZ, February 1982.

"Laser studies of state-selected chemical dynamics," Department of Chemistry Colloquium, University of Pittsburgh, Pittsburgh, PA, February 1982.

"Laser studies of state-selected chemical dynamics," Department of Chemistry Seminar, Kansas State University, Manhattan, KS, March 1982.

"Laser studies of state-selected chemical dynamics," American Chemical Society Meeting, Symposium for receipt of Pure Chemistry Award, Las Vegas, NV, March 1982.

"Laser studies of state-selected chemical dynamics," Department of Chemistry Seminar, University of Illinois at Chicago Circle, Chicago, IL, April 1982.

"Laser studies of state-selected chemical dynamics," Department of Chemistry Seminar, University of Illinois, Champagne, IL, April 1982.

"Laser studies of state-selected chemical dynamics," Department of Chemistry Seminar, Emory University, Atlanta, GA, May 1982.

"Laser studies of chemical reaction dynamics," Department of Chemistry Seminar, Yale University, New Haven, CT, September 1982.

"Laser studies of chemical reaction dynamics," Department of Chemistry Colloquium, The Pennsylvania State University, University Park, PA, September 1982.

"Laser studies of reactive dynamics," Harvard/MIT Seminar, Harvard University, Cmabridge, MA, October 1982.

S. R. Leone - Consulting

Consulting with S. Davis, Capt. D. Neumann . "Energy transfer and lasing in atomic calcium," Air Force Weapons Laboratory, Albuquerque, NM, February 1982.

Consulting with John Paulson, Ed Murad and Russ Armstrong. "Laser and infrared chemiluminescence studies of ion chemistry," Air Force Geophysics Laboratory, Hanscom Air Force Base, MA, October 1982.

G. Barney Ellison - Seminars and Conferences

"Ion Spectroscopy and Reaction Dynamics"

University of Wyoming, Jan. 30, 1979
Metropolitan State College (Denver), Dec. 14, 1979
Colorado State University, Dec. 17, 1979

University of Chicago, Oct. 31, 1980
University of Illinois (Urbana), Nov. 4, 1980
Washington University (St. Louis), Nov. 6, 1980
Wesleyan University (Middletown, CT), Dec. 2, 1980
Harvard University, Dec. 5, 1980
Joint Institute for Laboratory Astrophysics, Dec. 12, 1980

University of Denver, Feb. 3, 1981
Amherst College, Nov. 17, 1981
University of Pittsburgh, Nov. 19, 1981

The Johns Hopkins University, Feb. 9, 1982
University of Connecticut, Feb. 10, 1982
Yale University (Atomic Physics), Mar. 1, 1982
University of Oregon (Eugene), May 24, 1982

Second Annual NSF Workshop on Physical Organic Chemistry
(Co-Chairman), June 24-27, 1982